

The Jackson Laboratory

The Mouseion at the JAXlibrary

Faculty Research 2023

Faculty & Staff Research

7-25-2023

Cancer-associated mesothelial cells are regulated by the anti-Müllerian hormone axis.

M Chauvin

M-C Meinsohn

S Dasari

P May

S Iyer

See next page for additional authors

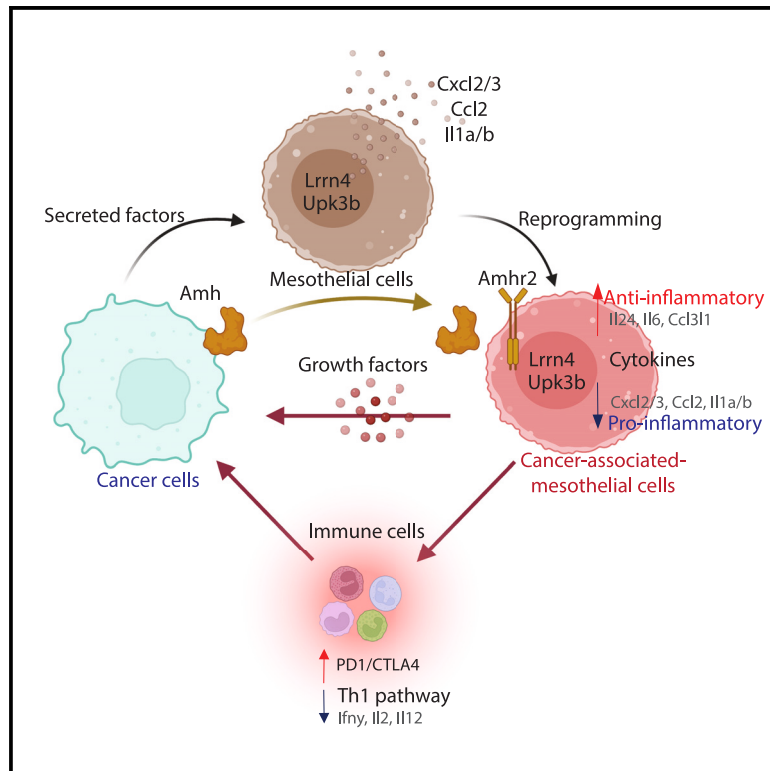
Follow this and additional works at: <https://mouseion.jax.org/stfb2023>

Authors

M Chauvin, M-C Meinsohn, S Dasari, P May, S Iyer, N M P Nguyen, E Oliva, Z Lucchini, N Nagykerly, A Kashiwagi, R Mishra, Richard S. Maser, Julie Wells, Carol J Bult, A K Mitra, Patricia K Donahoe, and D Pépin

Cancer-associated mesothelial cells are regulated by the anti-Müllerian hormone axis

Graphical abstract



Authors

M. Chauvin, M.-C. Meinsohn, S. Dasari, ..., A.K. Mitra, Patricia K. Donahoe, D. Pépin

Correspondence

DPEPIN@mgh.harvard.edu

In brief

Cancer cells reprogram normal omental mesothelium into cancer-associated mesothelial cells (CAMCs) by inducing expression of AMHR2. In turn, cancer cells secrete AMH to regulate expression of immunosuppressive cytokines and growth factors by CAMCs. Ovarian tumors implanted in transgenic mice deficient in AMHR2 have a slower growth and reduced immune exhaustion.

Highlights

- Cancer-cell-secreted factors reprogram normal omental mesothelial cells to induce AMHR2
- AMH secreted by cancer cells modulates cancer-associated mesothelial cell cytokines
- The paracrine AMH/AMHR2 axis regulates the pro-tumoral and immune functions of CAMCs
- Deletion of *Amhr2* in mesothelium reduces ovarian tumor growth and immune exhaustion



Article

Cancer-associated mesothelial cells are regulated by the anti-Müllerian hormone axis

M. Chauvin,^{1,2} M.-C. Meinsohn,^{1,2} S. Dasari,³ P. May,¹ S. Iyer,⁴ N.M.P. Nguyen,^{1,2} E. Oliva,⁵ Z. Lucchini,¹ N. Nagykerly,^{1,2} A. Kashiwagi,^{1,2} R. Mishra,⁴ R. Maser,⁶ J. Wells,⁶ C.J. Bult,⁶ A.K. Mitra,³ Patricia K. Donahoe,^{1,2} and D. Pépin^{1,2,6,7,*}

¹Pediatric Surgical Research Laboratories, Massachusetts General Hospital, Boston, MA, USA

²Department of Surgery, Harvard Medical School, Boston, MA, USA

³Indiana University School of Medicine-Bloomington, Indiana University, Bloomington, IN, USA

⁴Whitehead Institute for Biomedical Research, Cambridge, MA, USA

⁵Department of Pathology, Massachusetts General Hospital, Boston, MA, USA

⁶Mouse Genome Informatics, The Jackson Laboratory, Bar Harbor, ME, USA

⁷Lead contact

*Correspondence: DPEPIN@mgh.harvard.edu

<https://doi.org/10.1016/j.celrep.2023.112730>

SUMMARY

Cancer-associated mesothelial cells (CAMCs) in the tumor microenvironment are thought to promote growth and immune evasion. We find that, in mouse and human ovarian tumors, cancer cells express anti-Müllerian hormone (AMH) while CAMCs express its receptor AMHR2, suggesting a paracrine axis. Factors secreted by cancer cells induce AMHR2 expression during their reprogramming into CAMCs in mouse and human *in vitro* models. Overexpression of AMHR2 in the Met5a mesothelial cell line is sufficient to induce expression of immunosuppressive cytokines and growth factors that stimulate ovarian cancer cell growth in an AMH-dependent way. Finally, syngeneic cancer cells implanted in transgenic mice with *Amhr2*^{-/-} CAMCs grow significantly slower than in wild-type hosts. The cytokine profile of *Amhr2*^{-/-} tumor-bearing mice is altered and their tumors express less immune checkpoint markers programmed-cell-death 1 (PD1) and cytotoxic T lymphocyte-associated protein 4 (CTLA4). Taken together, these data suggest that the AMH/AMHR2 axis plays a critical role in regulating the pro-tumoral function of CAMCs in ovarian cancer.

INTRODUCTION

Anti-Müllerian hormone (AMH, also known as MIS: Müllerian inhibiting substance) is a member of the transforming growth factor β (TGF- β) superfamily of ligands that regulates sex differentiation by causing the regression of the Müllerian duct in males.^{1,2} AMH signals via the AMH type II receptor (AMHR2), which is expressed in a variety of tumors, including cervical, endometrial, and epithelial ovarian cancers, whose cells of origin all derive from the fetal Müllerian ducts.³⁻⁶

Based on the fetal role of AMH as a suppressor of Müllerian development and the purported expression of AMHR2 in high-grade serous ovarian cancer (HGSOC), whose cell of origin is fallopian tube epithelium, AMH had previously been proposed as a potential treatment for this disease.⁷ Supporting this hypothesis, studies from our group and others have shown that supraphysiological doses of AMH, achieved through the use of either recombinant protein or gene therapy, could inhibit HGSOC tumor growth,^{8,9} as do therapeutic therapies aimed at its receptor, AMHR2.^{3,10,11} Strikingly, and despite these observed anti-tumorigenic properties at high concentrations, AMH is secreted by a variety of cancer cell lines.¹² Paradoxically, we and others have recently shown that inhibiting AMH signaling using neutralizing antibodies could also have an anti-tumorigenic

effect, resulting in inhibition of proliferation, activation of apoptosis, and inhibition of epithelial-to-mesenchymal transition (EMT) in cancer cells.^{12,13} We also reported that AMH could activate a pro-survival EMT pathway in a non-small-cell lung cancer (NSCSL) model.¹⁴ Taken together, these data suggest the tumor-endogenous AMH/AMHR2 pathway may promote tumor growth at physiological concentrations; thus, we hypothesize that the pro-tumoral function of AMH may be disrupted therapeutically by either over-stimulation (supraphysiologic AMH) or inhibition (AMH-neutralizing antibody).

However, all studies evaluating AMH in ovarian cancer to date have used mouse models where ovarian carcinomas were not derived from fallopian tube epithelium (its cell of origin) or xenografts that did not recapitulate the full tumor microenvironment due to the immunodeficiency of the mouse hosts. To address these shortcomings, we recently generated new syngeneic mouse models of ovarian cancer, which were derived from C56Bl/6 fallopian tube epithelium and recapitulate human genetic mutations and copy number variations.¹⁵ One such model is the KRAS^{G12V}, P53^{R172H}, CCNE1-overexpressing, AKT2-overexpressing (KPCA) cell line recapitulating the histopathological properties of CCNE-1-amplified HGSOC tumors, which generally respond poorly to chemotherapy and have particularly poor prognoses.¹⁵ This fully immunocompetent



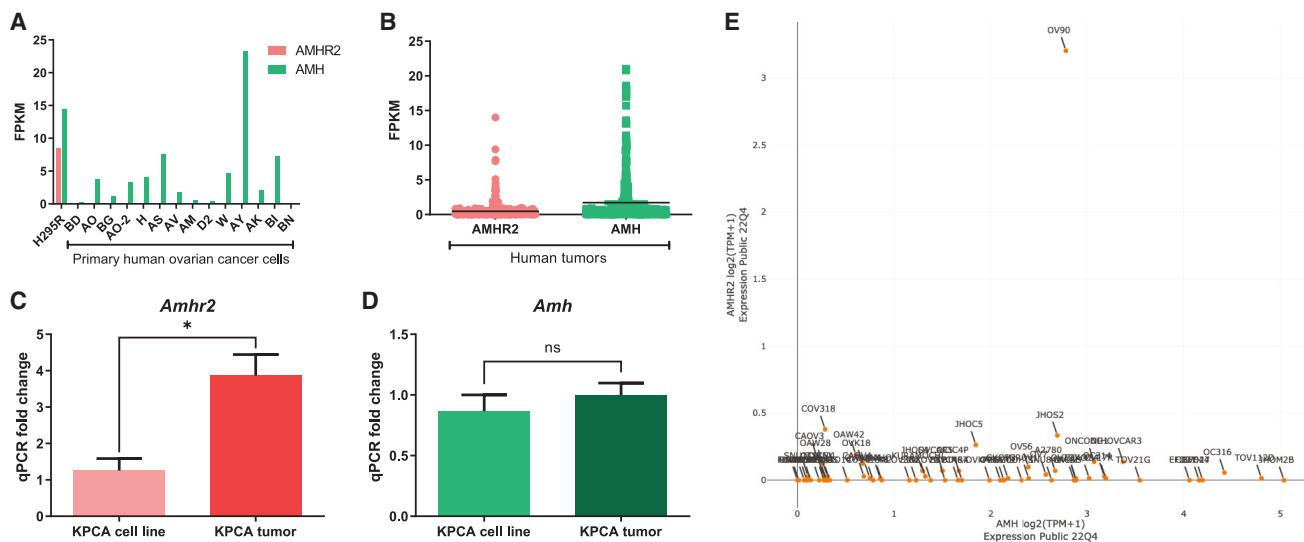


Figure 1. Expression of AMH and AMHR2 in human and mouse ovarian cancer

(A) A panel of 14 primary ovarian cancer cell lines derived from patient ascites cells were analyzed by bulk RNA-seq for expression of *AMHR2* and *AMH*, as quantified by fragments per kilobase million (FPKM). The adrenal carcinoma H295R is used here as a positive control for *AMHR2* and *AMH*.

(B–D) (B) Analysis of the TCGA dataset for *AMHR2* and *AMH* expression in $n = 373$ ovarian cancer tumors. Comparison of (C) *Amhr2* and (D) *Amh* expression by qPCR in the mouse ovarian cancer cell line (KPCA) and tumor resulting from engraftment of those cells in syngeneic hosts. Data are presented as mean \pm SEM; * $p < 0.05$, t test. $N = 5$ or more mice per group.

(E) Transcript levels of *AMH/AMHR2* in 62 common human ovarian cancer cell lines (log transformed transcripts per million [TPM] + 1) by bulk RNA-seq from the Broad Institute 22Q4 public expression profile dataset.

C57BL/6 syngeneic mouse model allowed us for the first time to study the role of AMH and its receptor AMHR2 in an ovarian tumor microenvironment that recapitulates many of the characteristics of HGSOCS arising in humans.

HGSOC tumors are heterogeneous, with many cell types contributing to chemoresistance and immune evasion, including cancer cells, cancer-associated fibroblasts (CAFs), vascular cells, immune cells, and cancer-associated mesothelial cells (CAMCs). The latter are thought to be derived from the mesothelium lining the peritoneal cavity, which normally plays a role in protecting visceral organs by producing serosal fluids. Additionally, mesothelial cells provide an important immune surveillance function in the peritoneum by regulating both innate and adaptive immune responses at the serosal surface by acting as antigen-presenting cells,¹⁶ responding to peritoneal pathogens,^{17–19} and interacting with cancer cells.²⁰ While mesothelial cells have been intensely studied in the context of peritoneal metastasis,^{18,21,22} where they represent the first point of contact of ovarian carcinoma cells when they disseminate,^{21,23–28} little is known about their subsequent contribution to the ovarian tumor microenvironment. Recent studies have suggested that CAMCs may play a direct role in supporting tumor growth by responding to TGF- β signals from cancer cells and secreting growth factors such as osteopontin (SPP1),²⁹ and also by contributing to immune evasion via antigen presentation and conversion of naive CD4⁺ T cells into regulatory T cells (Tregs).²⁰

Herein, we present evidence that factors secreted by ovarian cancer cells reprogram normal omental mesothelial cells into CAMCs and that this differentiation is accompanied by an induction of AMHR2 expression. Furthermore, we show that AMH,

which is produced by cancer cells, can regulate the expression of growth factors and immunomodulatory cytokines in AMHR2-bearing CAMCs. Conversely, deletion of *Amhr2* in the stroma of mouse hosts significantly reduces the growth of syngeneic KPCA tumors and produces a more immune-permissive tumor microenvironment.

RESULTS

AMH is expressed in cancer cells, while AMHR2 is expressed in CAMCs

To determine the level of expression of *AMH* and *AMHR2* in ovarian cancer cells, we analyzed their transcriptomic profile by bulk RNA sequencing (RNA-seq)³⁰ in a panel of 14 primary HGSOC cell lines previously isolated from patient ascites.^{9,31} We found that *AMH* expression was ubiquitous in primary ovarian cancer cells, whereas expression of its receptor, *AMHR2*, was notably absent (Figure 1A). This same pattern of expression was present in 62 epithelial ovarian cancer cell lines commonly used in the literature having nearly ubiquitous expression of AMH and absent expression of AMHR2, with the notable exception of OV90 (Figure 1E), when analyzing transcript abundance in the public 22Q4 RNA-seq dataset.³² In contrast, analysis of whole-tumor transcriptomes from The Cancer Genome Atlas (TCGA) dataset revealed the expression of *AMHR2* in a subset of ovarian cancer patients. Similarly, we assessed expression of *Amh* and *Amhr2* transcripts by qPCR in the KPCA murine ovarian cancer cell line: while *Amh* expression was high, we found only modest expression of *Amhr2*. In contrast, after implantation into syngeneic hosts, tumors that contained

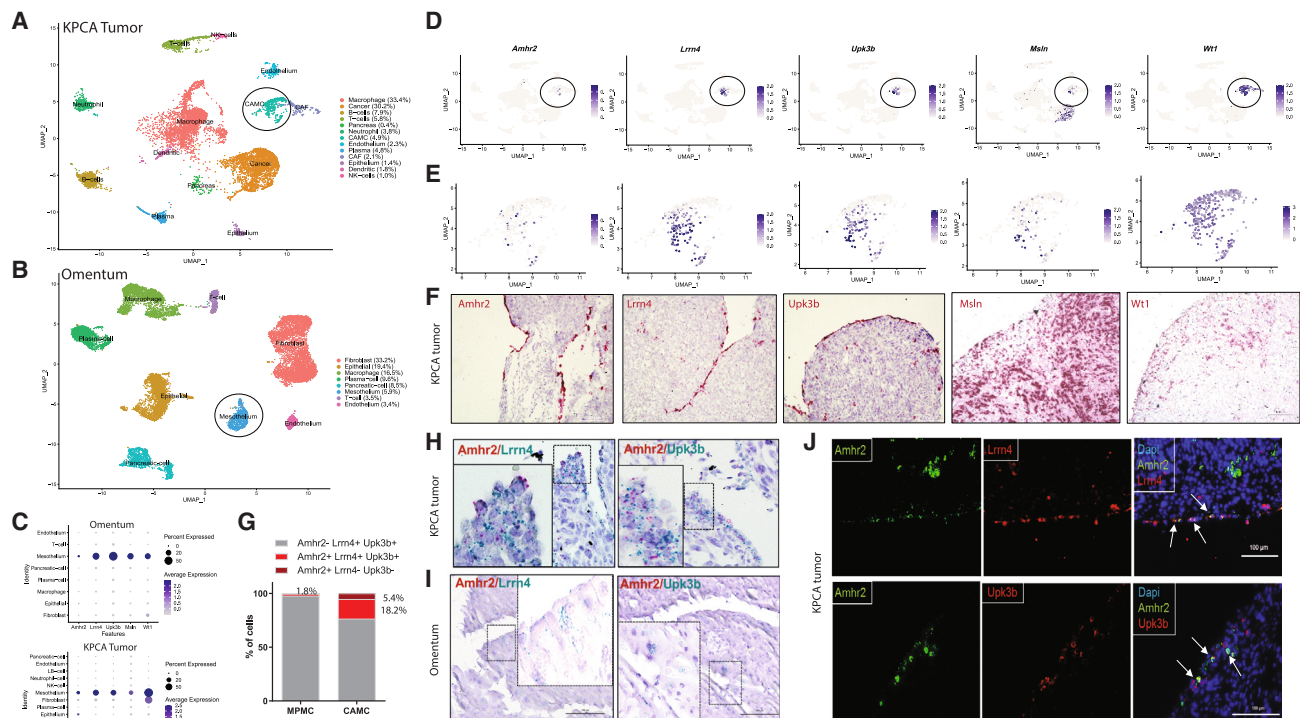


Figure 2. Expression of AMHR2 in cancer-associated mesothelial cells

(A and B) Uniform Manifold Approximation and Projection (UMAP) plot of scRNA-seq data from (A) pooled KPCA omental tumors, and (B) normal omentum (GSE134355)³⁸ clustered by cell type with the proportion of cells representing each cluster displayed. (C) Dot plot of expression of *Amhr2* and other mesothelial markers (*Lrrn4*, *Upk3b*, *Msln*, and *Wt1*) in clusters from scRNA-seq analyses of normal omentum and KPCA-derived omental metastases in mice. (D and E) UMAP feature plots in all clusters and (E) specifically in the mesothelial cluster of *Amhr2*, *Lrrn4*, *Upk3b*, *Msln*, and *Wt1*. (F) Representative micrographs of RNAish showing *Amhr2* and mesothelial markers *Lrrn4*, *Upk3b*, *Msln*, and *Wt1* at the surface of KPCA-derived omental metastases. (G) Proportion of cells co-expressing combinations of *Amhr2*, *Lrrn4*, and *Upk3b* in a normal mouse primary mesothelial cells (MPMC) from mouse omentum and in KPCA tumor in respective scRNA-seq datasets. (H and I) Co-expression of *Amhr2* and *Lrrn4* or *Upk3b* markers by RNAish in murine KPCA tumors and (I) in sections of normal omentum (red = *Amhr2*; blue = *Lrrn4*, *Upk3b*). (J) IF of co-expression of AMHR2/LRRN4 and AMHR2/UPK3B in KPCA tumor sections. Arrows highlight examples of co-expressing cells. Scale bars, 100 μ m.

both KPCA cancer cells as well as stromal cells from the host had significantly higher (>3 fold) expression of *Amhr2* compared to the KPCA cells from which they were derived (Figure 1C). However, *Amh* expression levels were similar both *in vitro* in the KPCA cell line and *in vivo* in tumors derived from this line (Figure 1D). Altogether, these data suggest that stromal cell types present in the tumor microenvironment are the major source of AMHR2 expression in mice and humans and that most ovarian cancer cells express AMH but little to no AMHR2.

To identify the putative stromal cell type(s) within the tumor microenvironment that express *Amhr2*, we performed single-cell RNA-seq (scRNA-seq) of tumors derived from the KPCA syngeneic mouse model. The KPCA cancer cells were implanted intraperitoneally into C57BL/6 mice and, 2 weeks later, omental tumors were harvested, dissociated, and analyzed by scRNA-seq (Figure 2A). Analysis of the scRNA-seq dataset identified multiple cell types within the tumor microenvironment, such as immunocytes, fibroblasts, endothelial cells, and mesothelial

cells, which could be identified by their unique gene signatures (Figure S1A). In the mesothelial cell cluster of tumors (CAMCs), representing 4.9% of the total tumor cell population, we detected *Amhr2* expression in 18.2% of cells, while *Amhr2* was expressed in only 1.8% of normal mouse omental mesothelial cells from dataset GSE134355 (Figure 2G). In the KPCA tumor, *Amhr2* expression coincided with other known mesothelial markers such as *Upk3b*, *Lrrn4*, *Wt1*, and *Msln*^{33–35} (Figures 2C, 2D, and 2E). We hypothesized that this *Amhr2*-positive cell population represented CAMCs, a stromal cell type thought to contribute to tumor growth and immune evasion.^{17,27,29,36,37}

To test this hypothesis, we evaluated the spatial distribution and marker expression of these putative *Amhr2*-positive CAMCs. We confirmed the presence of *Amhr2*-positive cells at the surface of the tumor, and sometimes invading into the tumor stroma (Figure 2F), which co-expressed the mesothelial cell markers *Upk3b* and *Lrrn4* as detected by RNA *in situ* hybridization (RNAish) and by immunofluorescence (IF), consistent with

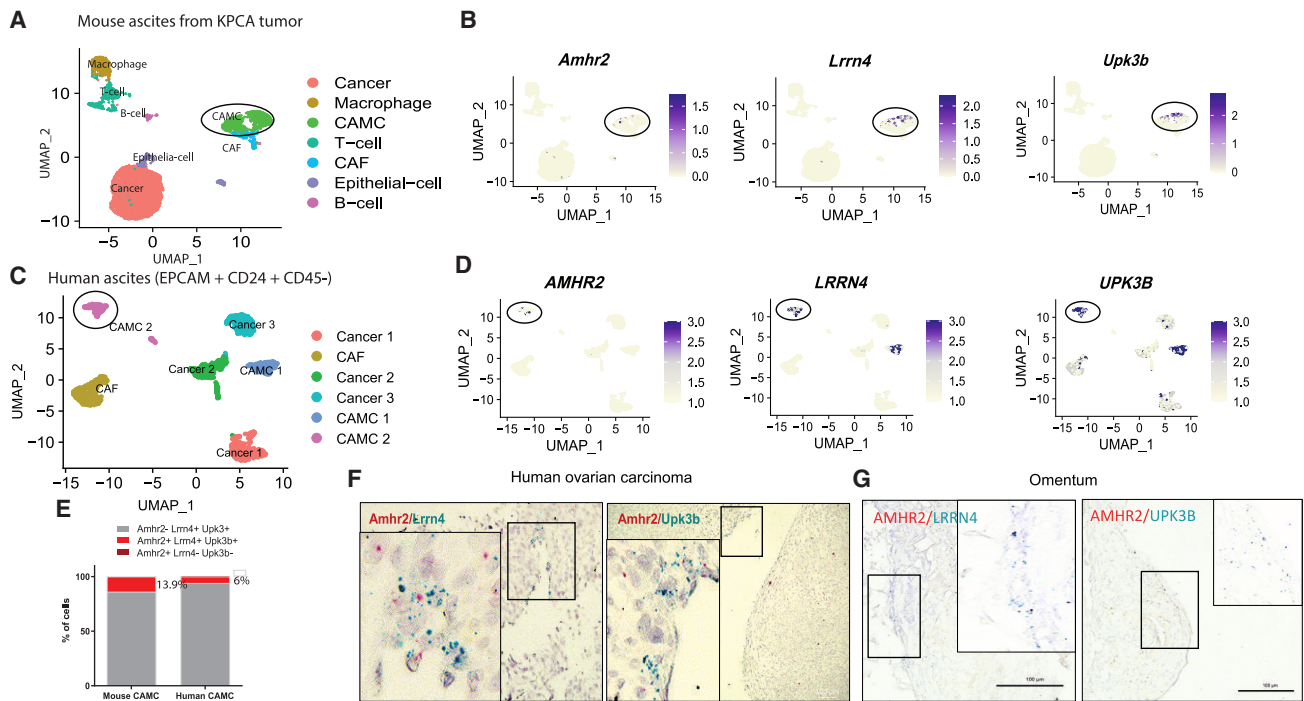


Figure 3. Expression of AMHR2 in CAMCs in mouse and human ovarian cancer ascites

(A and B) UMAP plot of clusters from scRNA-seq analysis of ascites of mice grafted with KPCA cells, and (B) corresponding FeaturePlot of expression of *Amhr2*, *Lrrn4*, and *Upk3b* markers in those clusters.

(C and D) UMAP plot of clusters from scRNA-seq analysis of human ascites samples depleted of CD45⁺ cells and sorted by EPCAM⁺CD24⁺CD45⁻, and (D) FeaturePlot of expression of *AMHR2*, *LRRN4*, and *UPK3B* markers in those clusters.

(E) Proportion of cells (%) co-expressing combinations of *Amhr2*, *Lrrn4*, and *Upk3b* in mouse and human ascites from their respective scRNA-seq datasets.

(F and G) Representative micrographs of RNAish showing co-expression of *AMHR2* and the mesothelial markers *LRRN4* and *UPK3B* in human high-grade serous tumors that metastasized to the omentum and (G) in section of normal human omentum (red: *Amhr2*; blue: *Lrrn4*, *Upk3b*). Rectangles show zoomed areas. Scale bars, 100 μ m.

the expected distribution and expression profile of CAMCs (Figures 2H and 2J). Importantly, unlike the mesothelial markers *Upk3b* and *Lrrn4*, *Amhr2* expression was rare in normal mouse omental sections; in contrast, these markers were often co-expressed in the context of omental metastases, suggesting *Amhr2* is greatly induced in cancer-associated mesothelium (Figure 2I). These findings were confirmed at the protein level by IF (Figure 2J). To examine the histological pattern of expression of *AMHR2* in human tumors, we performed RNAish of these same markers in five human HGSOE omental metastasis histological samples (Figure 3F). As observed in the KPCA mouse tumors, we identified a putative cancer-associated mesothelial cell type that co-expressed *AMHR2*, *UPK3B*, and *LRRN4* primarily at the tumor surface with some invasion of the tumor stroma, while *AMHR2* was rare or undetectable in normal human omentum (Figure 3G).

To see if expression of *AMHR2* in mesothelium was unique to the tumor environment or also present in the activated mesothelium found abundantly in ascites, we performed an scRNA-seq analysis of ascites cells collected at the time of tumor resection in the KPCA syngeneic model. We identified multiple cell types in the ascites microenvironment, such as immunocytes, cancer cells, CAFs, and CAMCs (Figure 3A). *Amhr2* expression was

again observed in 13.9% of mesothelial cells also expressing *Lrrn4*⁺ and *Upk3b*⁺ (Figure 3E). A similar pattern of expression was found in mesothelial cells of human ascites (sorted for EPCAM⁺, CD24⁺, and CD45⁻) from the patient dataset GSE146026,³⁹ where *AMHR2* was expressed in 6% of the *LRRN4*⁺ and *UPK3B*⁺ mesothelium found in those ascites (Figures 3C, 3D, and 3E).

Interestingly, outside of the context of tumors (Figure S2A), *Amhr2* is absent from Müllerian mesothelium and luminal epithelium in the mouse. Neither fallopian tube epithelium and mesothelium nor uterine epithelium and mesothelium express *Amhr2* (Figures S2B and S2C). In contrast, the mesothelial lining of the ovary, a frequent site of ovarian cancer metastasis, is unique in expressing *Amhr2*⁺, *Lrrn4*⁺, and *Upk3b*⁺, much like CAMCs (Figure S2A).

Cancer cells secrete factors that can reprogram normal mesothelial cells and induce a pro-tumoral cancer-associated mesothelial cell phenotype

We next sought to explore how cancer cells reprogram normal omental mesothelial cells into CAMCs, and particularly if they can induce *Amhr2* expression in normal mesothelial cells. To investigate this reprogramming *in vitro*, we dissociated cells

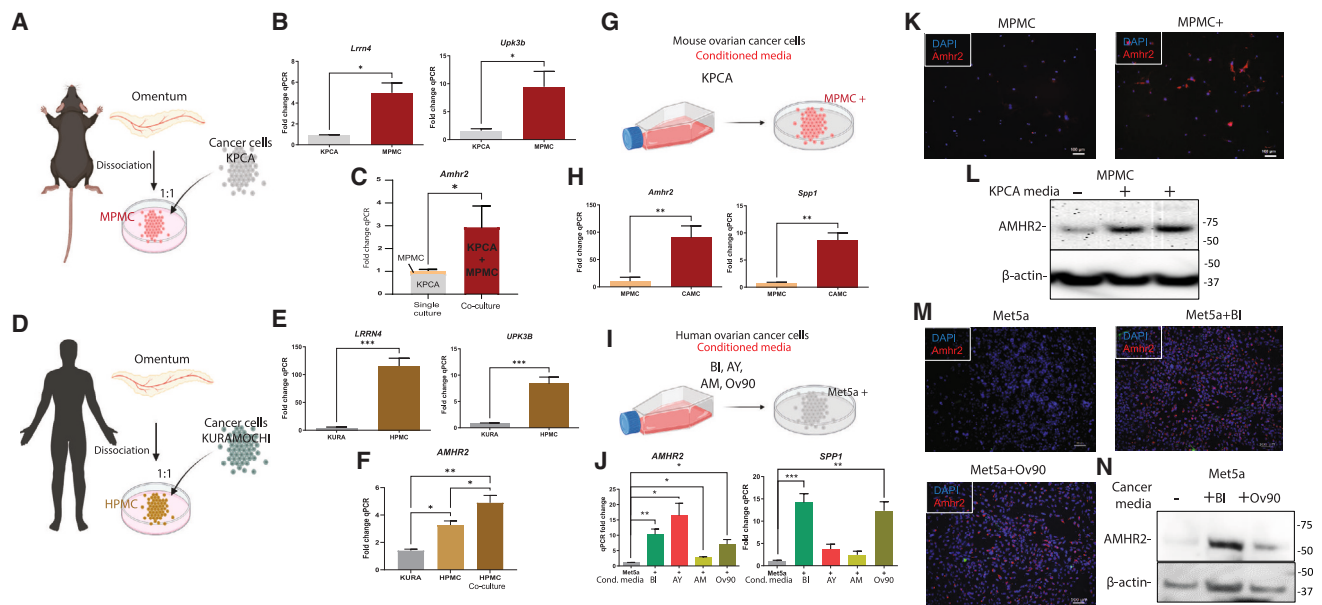


Figure 4. Cancer-cell-secreted factors can reprogram mesothelial cells into a CAMC phenotype

(A) Schema of the co-culture experimental design of mouse primary mesothelial cell (MPMC) dissociated from the omentum, co-cultured with murine cancer cells (KPCA).
 (B) Expression of mesothelial markers *Lrrm4* and *Upk3b* in cancer cells (KPCA) and isolated primary mesothelial cell cultures (MPMC).
 (C) Expression of *Amhr2* by qPCR in KPCA and normal MPMC and in co-cultures of the two, normalized for a mixing ratio of 1:1.
 (D) Schema of the co-culture experimental design of human primary mesothelial cells (HPMCs) dissociated from the omentum, co-cultured with a human ovarian cancer cell line (KURA, Kuramochi).
 (E) Expression of mesothelial markers *LRRN4* and *UPK3B* in cancer cells (KURA) and human primary mesothelial cells (HPMC).
 (F) Expression of *AMHR2* by qPCR in co-cultures of the human ovarian cancer cell line (KURA) and normal human primary omental mesothelial cells (HPMC), at a ratio of 1:1, with the HPMCs isolated by flow cytometry after co-culture (HPMC co-culture).
 (G) Schema of the experimental design of MPMC treated with KPCA cancer-cell-conditioned medium.
 (H) The effect of KPCA-conditioned medium (48-h conditioning) on the expression of *Amhr2* and the CAMC marker *Spp1* in treated MPMCs quantified by qPCR at 48 h (n = 3 experiments).
 (I) Schema of the experimental design of treatment of the human mesothelial cell line *Met5a* with various human HGSOc cancer-cell-conditioned media (BI, AY, AM).
 (J) The effect of medium conditioned (for 24 h) by human primary ovarian cancer cells (BI, AY, AM) or a human ovarian cancer cell line (OV90) on the expression of *AMHR2* and *SPP1* in *Met5a* as quantified by qPCR at 72 h (n = 3 experiments).
 (K and L) *AMHR2* expression in control MPMCs and MPMCs treated with KPCA-conditioned medium (MPMC+) for 48 h by IF and (L) western blot (β -actin as loading control).
 (M and N) Expression of *AMHR2* in *Met5a* stimulated with BI and OV90 cancer-cell-conditioned medium by IF and by (N) western blot (β -actin as loading control). Data are presented as mean \pm SEM; *p < 0.05, **p < 0.01, ***p < 0.001 by t test. n = 3 or more per group. Scale bars, 100 μ m.

enzymatically from the omenta of healthy mice using a protocol previously used to create cultures of mouse primary mesothelial cells (MPMCs) (Figure 4A).^{40,41} We verified that those cells expressed the specific mesothelial markers *Lrrm4* and *Upk3b* (Figure 4B) and co-cultured them with an equal number of KPCA murine ovarian cancer cells (Figure 4A). We found that, while normal omental mesothelial cells expressed very low amounts of *Amhr2* when cultured alone, co-culture with cancer cells significantly increased its expression (Figure 4C).

Similarly, we performed a co-culture experiment using the human HGSOc cell line Kuramochi (KURA), which was transfected with GFP and mixed 1:1 with normal human primary mesothelial cells (HPMCs) isolated from the normal omenta of patients (Figure 4D), as previously described.^{40,41} Again, the human mesothelial cells were confirmed to express the mesothelial markers *UPK3B* and *LRRN4* by qPCR (Figure 4E). Following co-culture, the two cell types were separated by fluorescence-

activated cell sorting (FACS) based on the GFP fluorescence introduced into Kuramochi cells, and gene expression was analyzed separately in each cell type by qPCR. *AMHR2* expression in co-cultured HPMC was 10-fold higher than in Kuramochi cancer cells and significantly higher than in non-co-cultured mesothelial cells (Figure 4F). Therefore, we concluded that co-culture of cancer cells with normal omental mesothelial cells was sufficient to induce *AMHR2* expression and speculated that *AMHR2* may represent a marker of CAMC differentiation.

To investigate if the reprogramming of mesothelial cells is mediated by physical interaction with, or paracrine signaling from, cancer cells, we evaluated the ability of cancer-cell-conditioned medium (cell-free) to induce *Amhr2* expression in normal mesothelial cells (Figure 4G). We conditioned medium with KPCA cancer cells propagated in monolayer culture for 24 h and used it to treat MPMCs for 72 h (Figure 4G), the time point of maximal induction (Figure S3A). KPCA-conditioned medium

significantly induced *Amhr2* transcript expression (>50 fold) in the mouse mesothelial cells as measured by qPCR, along with osteopontin (*Spp1*), a marker previously identified in CAMCs²⁹ (Figure 4H). However, the condition medium did not significantly change expression of normal mesothelial markers *Upk3b* and *Lrrn4* (Figure S3B). The induction of AMHR2 by KPCA-conditioned medium was also confirmed at the protein level by IF and western blot in MPMCs treated for 72 h (Figures 4K and 4L) and was accompanied by induction of p-SMAD1, suggesting induction of AMH/AMHR2 signaling in these cells (Figure S3C).

To investigate if human cancer cells also secrete factors that can reprogram human mesothelial cells, we performed a similar experiment (Figure 4I) using Met5a, an immortalized lung mesothelial cell line, cultured in presence of medium conditioned by human primary ovarian cancer cells from deidentified patients (coded as BI, AY, AM) negative for AMHR2, or by an established human cancer cell line (OV90) positive for AMHR2 (Figure 4I). As in mice, human-cancer-cell-conditioned medium were sufficient to induce significant upregulation *AMHR2* in Met5a for all samples and produced a trend for increased *SPP1* (significant for BI and OV90) (Figure 4J), while treatments had no significant effects on expression of the mesothelial markers *UPK3B* and *LRRN4* (Figure S3E). The induction of AMHR2 by BI and OV90-conditioned medium was also confirmed at the protein level by IF and western blot on Met5a treated for 72 h (Figures 4M and 4N).

Taken together, these data suggest factors secreted by cancer cells can reprogram normal mesothelial cells (LRRN4+, UPK3B+, SPP1-, AMHR2-) into CAMCs and that this differentiation is associated with an induction of AMHR2 expression (LRRN4+, UPK3B+, SPP1+, AMHR2+).

To determine the fate of the CAMC cells following AMHR2 induction, we developed a transgenic mouse with a Cre recombinase (Cre)-estrogen receptor (ER) fusion expressed under the control of the AMHR2 promoter (*Amhr2*-Cre-ERT2) (Figure S3F). This transgenic reporter model was produced by inserting a Cre-ER fusion in the *Amhr2* locus, replacing the stop codon with a 2A ribosomal skipping site so that Cre-ER could be produced in tandem with AMHR2. This tamoxifen-inducible Cre mouse model was crossed with mice carrying the fluorescent mTmG reporter allele in the *Rosa26* locus,^{42,43} which conditionally converts the locus from the tdTomato to mGFP reporter gene permanently in *Amhr2*-expressing cells and their descendants (Figure S3F). We then tracked the AMHR2+ cells and their descendants in normal omenta and during tumor growth in mTmG mice and identified the lineage of CAMCs (green cells) at the surface of the omentum only in the presence of tumors (Figure S3G), at the surface of the tumor, and integrated into the tumor microenvironment (Figure S3H).

To determine if the differentiation of mesothelial cells into CAMCs is terminal or if CAMCs can proliferate, we performed a similar *in vitro* lineage tracing experiment (Figure S3I). We harvested mesothelial cells from the omenta of *Amhr2*-Cre^{+/+}, mTmG^{+/+} mice, and treated them *in vitro* with KPCA-conditioned medium (or fresh control medium), concurrently with tamoxifen (2 μ M). After 48 h of tamoxifen treatment, we were able to detect GFP+ cells only in the omental mesothelial cell cultures treated with the cancer-cell-conditioned medium, often in tight flattened

mesothelial-like colonies (Figure S3I). Taken together, these data suggest AMHR2 is not expressed by normal mesothelial cells in culture; however, following reprogramming by cancer-cell-secreted factors, the AMHR2+ CAMCs form colonies in culture.

Ectopic overexpression of *Amhr2* in normal mesothelial cells induces a CAMC-like phenotype

To understand how AMHR2 itself might contribute to the reprogramming of mesothelial cells into a cancer-associated phenotype, we transfected Met5a cells,⁴⁴ a normal human immortalized mesothelial cell line that does not normally express AMHR2, to overexpress an active (V1) or dominant-negative (V3) *AMHR2* splice variant together with the type I co-receptor *ACVR1*⁴⁵ on a T2A co-expression construct to ensure full reconstitution of AMH receptor signaling (Figure 5A). We validated overexpression of AMHR2 variant transcripts by qPCR (Figure 5C) and proteins by IF (Figure 5D) and western blot (Figure 5B). Only Met5a cells transfected with the active *AMHR2v1* gene also induced expression of *AMH*, suggesting the activation of an AMH/AMHR2 autocrine positive-feedback loop (Figure 5C). Overexpression of AMHR2 did not alter the cytoskeletal appearance (VIM, ACTA2) or mitosis (KI67) by IF but did induce an upregulation of its downstream target p-SMAD1 by western blot, likely because of a constitutive AMH/AMHR2 feedback loop (Figure 5B).

To catalog how expression of AMHR2 may alter the transcriptome of mesothelial cells, we compared the transcriptional profiles of parental Met5a- and AMHR2-overexpressing Met5a clones by bulk RNA-seq. Comparing the transcriptomes of parental Met5a control cells to three clones overexpressing *AMHR2v1+ACVR1* identified genes differentially expressed based on expression of both type II and type I receptors. Comparing three clones overexpressing the dominant-negative *AMHR2v3+ACVR1* to those expressing the active *AMHR2v1+ACVR1* identified genes uniquely dependent on AMHR2 signaling, controlling for the effect of *ACVR1*, which is shared by other TGF- β superfamily type II receptors. By analyzing transcriptomes using bulk RNA-seq, we find 653 and 1,086 differentially expressed genes respectively for both comparisons, with a 16.2% overlap of genes (Figure 5F and Table S1). Interestingly, overexpression of *AMHR2v1* induced profound changes in the transcriptome of Met5a cells, particularly in genes significantly enriched as part of pathways, such as immunomodulatory cytokines and growth factors regulating the mitogen-activated protein kinase (MAPK) and TGF- β (Figure 5G). Select cytokine and growth factor genes were chosen for validation by qPCR (Figure 5H). We observed that overexpression of *AMHR2v1* in mesothelial cells significantly reduced the expression of pro-inflammatory cytokines involved in innate immunity, such as the chemoattractant *CCL2*,⁴⁶ *CXCL2*,⁴⁷ *CXCL3*,⁴⁸ and interleukins (ILs) *IL1A* and *IL1B*,⁴⁹⁻⁵¹ and increased the expression of immunosuppressive cytokines *IL6*,⁵²⁻⁵⁵ *IL20*, and *IL24*⁵⁶ (Figure 5H). Of particular interest were the differentially expressed genes related to the TGF- β superfamily (*BMP7*, *INHBB*, *INHBA*, *FSTL3*) and the induction of the growth factor osteopontin (*SPP1*), a factor previously reported to be regulated by TGF- β in CAMCs²⁹ (Figures 5E and 5H).

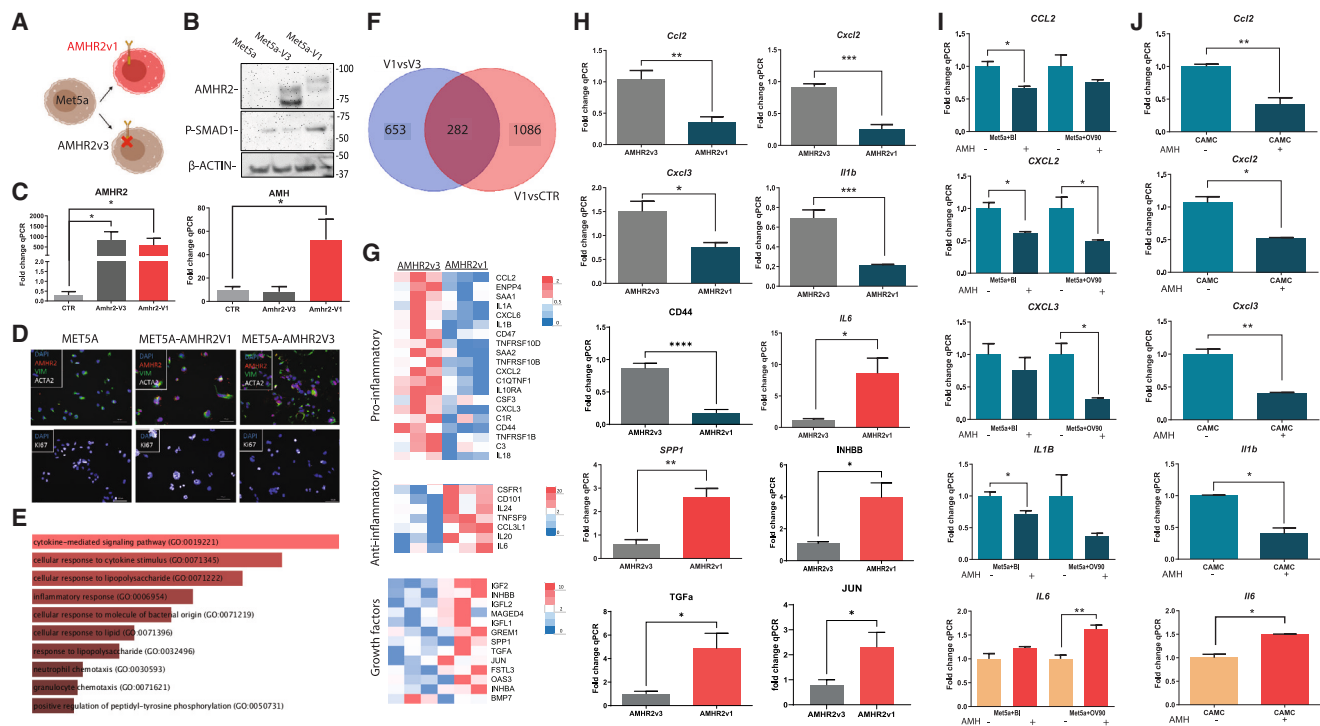


Figure 5. Overexpression of AMHR2 induces a CAMC-like transcriptional signature in normal mesothelial cells

(A) Experimental schema representing the generation of Met5a cell line clones stably expressing an active (V1) or dominant-negative (V3) splice variant of AMHR2 in conjunction with *ACVR1* (n = 3 clones per group).

(B) Western blot showing AMHR2 and p-SMAD1 expression in Met5a, Met5a-AMHR2v1, and Met5a-AMHR2v3.

(C) Expression of *AMHR2* and *AMH* in Met5a clones (*AMHR2v1*, *AMHR2v3*) and parental control (CTR) by qPCR.

(D) Confirmation of overexpression of AMHR2 by IF.

(E) Bar plot of significantly enriched GO terms in differentially expressed genes from bulk RNA-seq comparison of Met5a-AMHR2v1 and Met5a-AMHR2v3 clones (n = 3 per group).

(F) Venn diagram comparing the overlap of differentially expressed genes in *AMHR2v1* versus *AMHR2v3* (V1vsV3) and *AMHR2v1* versus parental control (V1vsCTR).

(G) Heatmap of differentially expressed genes regulated by AMHR2 expression in Met5a related to immune response and growth factors.

(H) qPCR validation of differentially expressed genes identified from RNA-seq in Met5a-AMHR2v1 and Met5a-AMHR2v3 clones, with downregulated genes in blue and upregulated genes in red.

(I) Validation of key AMHR2-regulated cytokine genes by qPCR in Met5a stimulated to differentiate into CAMCs by incubation with medium conditioned by human primary ovarian cancer cells (BI) or a human cancer cell line (OV90) and further treated with 10 $\mu\text{g}/\text{mL}$ of AMH (+) or vehicle control (-).

(J) qPCR validation of the mouse orthologs of those same regulatory cytokines in MPMCs stimulated to differentiate into CAMCs by incubation with medium conditioned by KPCA cancer cell line and further treated with 10 $\mu\text{g}/\text{mL}$ of AMH (+) or vehicle control (-). Data are presented as mean \pm SEM; *p < 0.05, **p < 0.01, ***p < 0.001 by t test. n = 3 or more per group. Scale bars, 100 μm .

We hypothesized that induction of AMHR2 expression in CAMCs allows cancer cells to, in turn, use AMH to dynamically regulate the cytokine and growth factor secretions of CAMCs. We therefore sought to determine if the cytokine genes identified as regulated by AMHR2 in mesothelial cells could be further modulated by exogenous AMH. Indeed, experimental overexpression of AMHR2 alone was sufficient to induce an AMH auto-crine loop in the Met5a mesothelial cells, suggesting cytokine gene expression may be dependent not only on the presence of AMHR2 protein but also on its signaling (Figures 5B and 5C), and ovarian cancer cells also produce additional AMH, which could further amplify this pathway (Figure 1A, 1D, and 1E). We therefore stimulated the Met5a human mesothelial cells to differentiate them into CAMCs with medium conditioned by BI and OV90 cancer cells, since these treatments induced the

strongest *SPP1* upregulation, a marker of CAMCs (Figure 3H). We then treated these CAMCs with exogenous recombinant AMH ligand at 10 $\mu\text{g}/\text{mL}$ (AMH+) or vehicle control (AMH-) (Figure 5I), then examined the expression of a panel of cytokine genes identified as AMHR2v1 dependent in these cells: *CCL2*, *CXCL2*, *CXCL3*, *IL1B*, and *IL6* (Figure 5H). Similarly, we evaluated the effect of exogenous recombinant AMH ligand on the murine MPMCs differentiated into CAMCs using KPCA-conditioned medium (Figure 5J). Interestingly, in both the human CAMCs reprogrammed by either BI or OV90 medium and the murine CAMCs reprogrammed by KPCA medium, the addition of exogenous AMH ligand could further suppress the expression of chemoattractant cytokines (*CCL2*, *CXCL2*, *CXCL3*, *IL1B*) and increase the expression of the immunosuppressive cytokine *IL6* (Figures 5I and 5J). These experiments suggest that, in tumors,

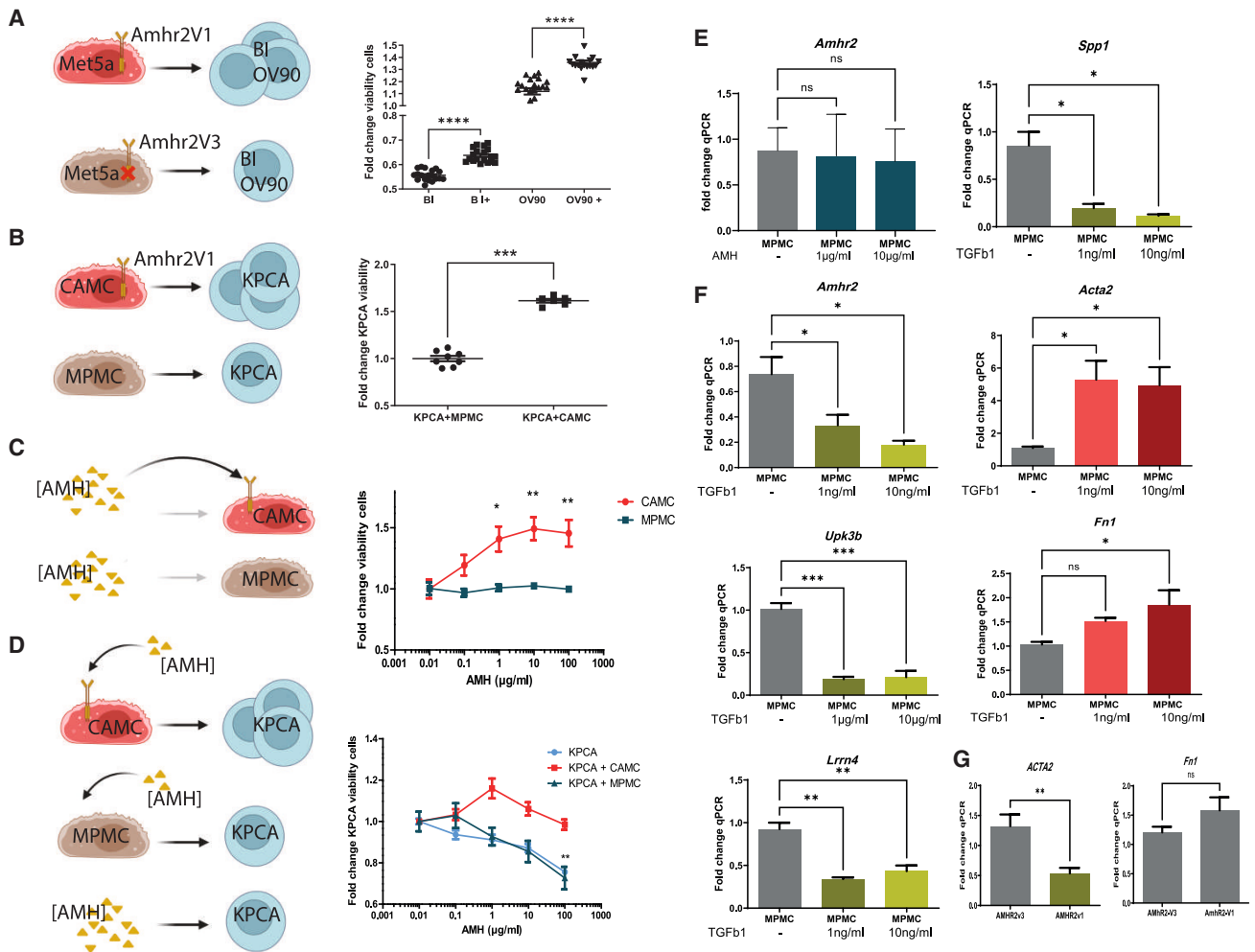


Figure 6. Effect of AMH on CAMCs and cancer-cell proliferation/viability and effect of AMH and TGF-β on MPMC reprogramming

(A) Growth of BI and Ov90 cells over 72 h following stimulation with medium conditioned by Met5a-AMHR2v1 or AMHR2v3 clones during 48 h as assessed by the CellTiter-Glo assay.

(B) KPCA cell growth/viability over 72 h following stimulation with conditioned medium from MPMCs and CAMCs (48 h) by CellTiter-Glo assay.

(C) Viability/growth of MPMCs and CAMCs at 72 h following treatment with 0, 0.1, 1, 10, and 100 μg/mL of AMH.

(D) Viability of KPCA stimulated with AMH or conditioned medium from MPMCs and CAMCs treated with AMH at 0, 0.1, 1, 10, and 100 μg/mL at 72 h by CellTiter-Glo assay.

(E) Expression of *Amhr2* at 72 h in MPMCs following treatment with 1 μg/mL or 10 μg/mL of recombinant AMH.

(F) qPCR of MPMC treated with 1 or 10 ng/mL of TGF-β1 during 48 h showing expression of CAMC (*Amhr2*), mesothelial (*Lrrn4*, *Upk3b*), and fibroblast (*Fn1*, *Acta2*) markers.

(G) Expression of *Fn1* and *Acta2* by qPCR in Met5a-AMHR2v1 and Met5a-AMHR2v3 clones. Data are presented as mean ± SEM; *p < 0.05, **p < 0.01, ***p < 0.001 by t test. n = 3 or more experiments per group.

the CAMC cytokine profile may be dynamically modulated by paracrine AMH secretions from cancer cells to promote an immunosuppressive tumor microenvironment.

CAMC secretions promote cancer cell growth but TGF-β inhibits the expression of CAMC markers

Another presumed pro-tumoral function of CAMCs is the secretion of growth factors. Having identified several growth factors (such as *SPP1*) whose expression could be induced by AMHR2 overexpression in Met5a, we sought to evaluate if the CAMC secretome could enhance cancer-cell proliferation and

viability and how AMH may further modulate this effect dose dependently. We therefore compared the effect of Met5a-AMHR2v1-conditioned medium to that of Met5a-AMHR2v3 (inactive variant control) on human primary HGSOc cells (BI) and on an established cell line (OV90). Remarkably, medium conditioned by Met5a cells (for 48 h) overexpressing AMHR2v1 significantly increased cancer cell viability after 72 h of growth compared to medium conditioned by Met5a overexpressing the catalytically inactive AMHR2v3 splice variant as assessed by the cell CellTiter-Glo luminescence assay (Figure 6A). The same effect was observed for medium conditioned by MPMCs

or CAMCs for 48 h and used to treat KPCA cells for 72 h, resulting in significantly increased viability of cancer cells in response to CAMC- but not MPMC-secreted factors (Figure 6B). To understand better the dose-dependent function of AMH in modulating the pro-tumoral secretome of CAMCs, we sought to compare the effect of AMH on MPMCs and CAMCs. Unsurprisingly, recombinant AMH had no effect on MPMCs, which do not express its receptor, while treatment of CAMCs with AMH at the 1–100- $\mu\text{g}/\text{mL}$ range significantly increased their viable cell growth at 72 h (Figure 6C). We next sought to evaluate if AMH could modulate the proliferative effect of CAMC-secreted factors on cancer cells. For this, we treated both MPMCs and CAMCs with a range of concentrations of recombinant AMH (0–100 $\mu\text{g}/\text{mL}$) for 48 h and then used this conditioned medium (still containing AMH and mesothelial-secreted factors) to treat KPCA cancer cells (Figure 6C). We found that, at low concentrations, AMH treatment further enhances the pro-cancer cell effects of CAMC-conditioned medium as measured by viability after 72 h of growth, but that this effect diminishes as concentrations of AMH are increased beyond 1 $\mu\text{g}/\text{mL}$ (Figure 6D). Furthermore, both the AMH-treated MPMC-conditioned medium and just the recombinant AMH alone significantly inhibited KPCA cell viability in a dose-dependent way (Figure 6D), suggesting supraphysiological AMH directly inhibits KPCA cancer cells, which express modest levels of AMHR2 (Figure 4C). Together, these data suggest low levels of AMH in the tumor microenvironment (~ 1 $\mu\text{g}/\text{mL}$) can enhance the pro-tumoral function of CAMCs, while high levels (~ 100 $\mu\text{g}/\text{mL}$) both suppress this function and inhibit KPCA cancer cells directly, providing a plausible mechanistic explanation of the paradoxical dose-dependent effect of AMH in ovarian tumors.^{12,13} More broadly, these data support the hypothesis that secretion of AMH by cancer cells can modulate AMHR2 activity in CAMCs, which in turn regulates the secretion of pro-tumoral factors that can enhance cancer-cell proliferation and viability.

Others have previously reported that the TGF- β pathway may also regulate the pro-tumoral function of CAMCs.²⁹ To examine if the mesothelial cell reprogramming into CAMCs occurs by cancer-cell secretions, and the regulation of cytokines and growth factors such as SPP1 may be due to an induction of the TGF- β pathway by AMHR2, we evaluated the effect of recombinant TGF- β on normal omental mouse mesothelial cell cultures. As expected, given the lack of expression of AMHR2 in normal MPMCs, recombinant AMH does not induce *Amhr2* expression in these cells (Figure 6E). Interestingly, treatment with recombinant TGF- β at 1 and 10 ng/mL suppressed *Amhr2* and *Amh*, and it inhibited *Spp1* and mesothelial markers *Lrrm4* and *upk3b*, while increasing known targets such as *Acta2* and *Fn1*⁵⁷ (Figure 6F), which were decreased or unchanged by *Amhr2* overexpression respectively (Figure 6G). Taken together, these data suggest that mesothelial cell reprogramming into CAMCs and induction of AMHR2 expression in our model cannot be recapitulated by AMH or TGF- β alone. However, TGF- β may provoke EMT of normal mouse omental mesothelial cells and loss of expression of mesothelial markers, including *Lrrm4*, *Upk3B*, *Amhr2*, and *Spp1*.

Expression of *Amhr2* in cancer-associated mesothelium is required for its pro-tumoral function

To test if *Amhr2* expression in the tumor stroma contributes to the growth of KPCA tumors, we took advantage of the fact that KPCA cells (which are wild type for their *Amhr2*^{+/+} alleles [CON]) can be implanted into a syngeneic C57Bl/6 *Amhr2*^{-/-} knockout (KO) mouse host.⁵⁸ Specifically, we compared tumors derived from KPCA cells implanted into either *Amhr2*^{-/-} KO mice or *Amhr2*^{+/+} CON control hosts, allowing us to evaluate the effect of loss of *Amhr2* expression in the stroma on tumor growth. Provocatively, KPCA cells implanted into *Amhr2*^{-/-} host (N = 10) produced a significantly reduced tumor burden compared to those implanted into *Amhr2*^{+/+} CON mice (N = 12) counterparts after 2 weeks (Figure 7A). This difference was also accompanied by a significant reduction of non-omental metastatic nodules (Figures 7B and 7C). We could still detect *Lrrm4*+ *Upk3b*+ mesothelial cells on the surface of tumors growing in *Amhr2*^{-/-} hosts, but, as expected, these mesothelial cells failed to express *Amhr2* by RNAish (Figure 7D).

To determine if the failure to express *Amhr2* in CAMCs could alter the secretome of ovarian tumors, we measured cytokines in the serum of *Amhr2*^{+/+} CON and *Amhr2*^{-/-} KO mice 10 days after implantation of KPCA cells. A cytokine array revealed a trend for increases in the stimulatory cytokines IL2,⁵⁹ IL12p70,⁶⁰ and interferon γ (IFN γ),⁶¹ involved in the stimulation of the T helper 1 (Th1) pathway, which activates T helper CD4+ cells. Moreover, we found a significant increase in CCL3, a macrophage chemoattractant,⁶² and a significant decrease in IL16, a cytokine known to preferentially activate the Th2 pathway,⁶³ in *Amhr2*^{-/-} tumor-bearing hosts (Figure 7E). We hypothesized that these altered cytokines may be the cause and/or consequence of differential recruitment of immunocytes to these tumors, as shown by a trend for increased expression of markers of dendritic cells (CD11c) and B cells (CD20) in the bulk RNA-seq generated from *Amhr2*^{+/+} and *Amhr2*^{-/-} omental tumors (Figures S4A and S4B). Moreover, we found a significant reduction of expression of the immune checkpoint protein PD1, and a trend for a reduction of cytotoxic T lymphocyte-associated protein 4 (CTLA4) expression, in the *Amhr2*-KO tumors (Figure S4B).

We therefore hypothesized that loss of *Amhr2* expression in mesothelial cells could alter the cytokine secretome of the tumor and produce a more immunogenic tumor immune microenvironment. To test this hypothesis, we evaluated expression of the immunosuppressive checkpoint proteins PD1 and CTLA4 in the KPCA tumors of *Amhr2*^{+/+} CON and *Amhr2*^{-/-} KO hosts by IF and found drastically reduced staining of these proteins in tumors of *Amhr2*^{-/-} KO animals (Figure 7F). These findings were further supported by evidence of significantly reduced abundance of the corresponding transcripts (normalized by CD4+ transcript abundance) by qPCR. Gene Ontology (GO) enrichment analysis of differentially expressed genes in tumors of *Amhr2*^{+/+} CON and *Amhr2*^{-/-} KO hosts were significantly enriched for T cell-related GO pathways (Figure S4C and Table S2).

Taken together, these data suggest that *Amhr2*^{-/-} CAMCs have a reduced pro-tumoral function *in vivo* compared to their WT counterparts, leading to a less immunosuppressive cytokine profile and a reduction in immunosuppressive T cell infiltration and resulting in a significantly decreased tumor burden. We

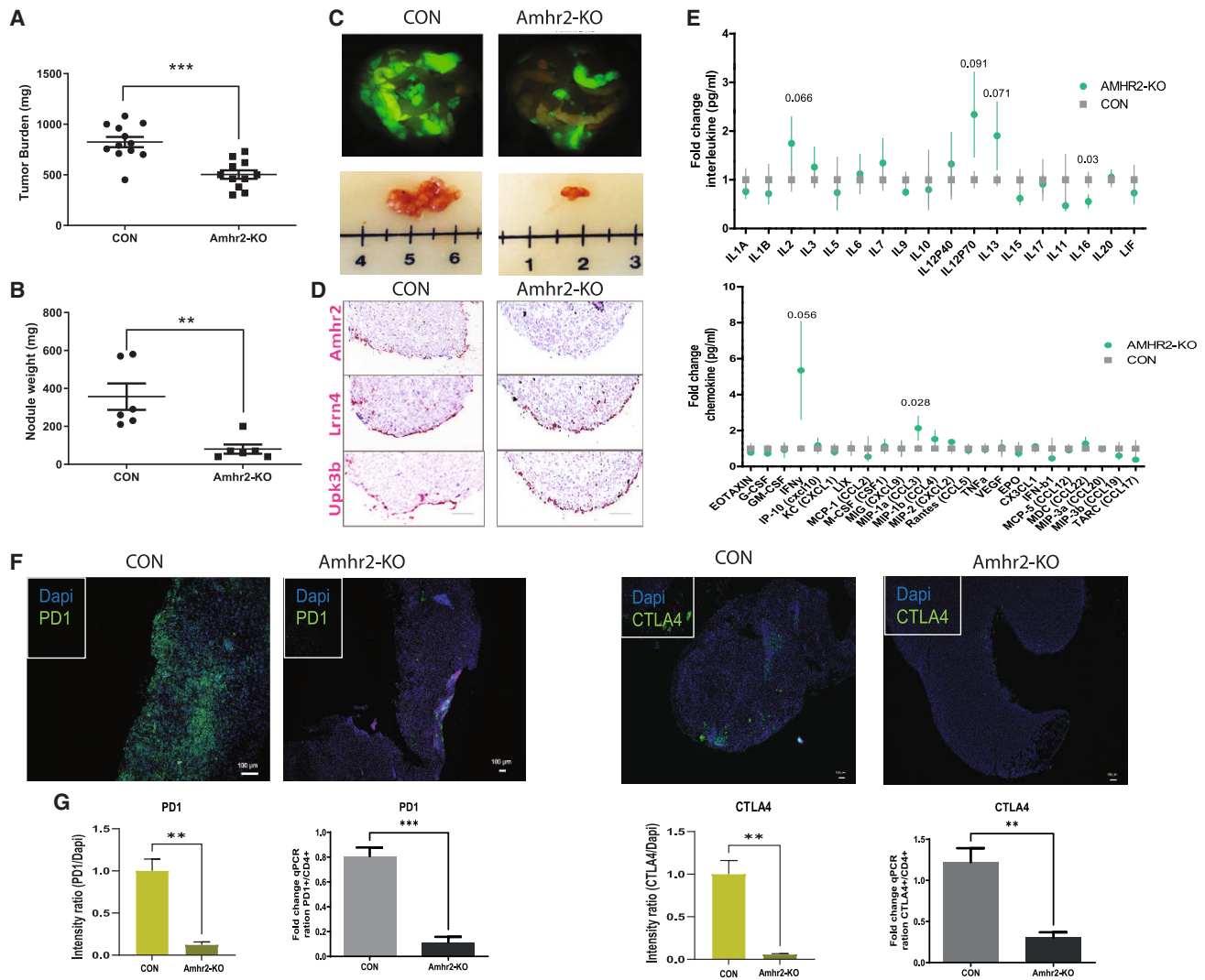


Figure 7. Loss of AMHR2 expression in the tumor stroma suppresses tumor growth and immune evasion

(A and B) Tumor burden from mice implanted with KPCA cells in *Amhr2*^{-/-} KO mice (*Amhr2*-KO) compared to controls (CON), and (B) total peritoneal (non-omental) nodule weight in AMHR2-KO mice compared to controls (CON). Data are presented as mean ± SEM; **p < 0.01, ***p < 0.001, t test. n = 5 or more/group. Each dot represents tumor weight from a mouse.

(C) Micrograph of KPCA cancer-cell GFP+ fluorescence in peritoneal tumors. Scale bars, 1 cm.

(D) Representative peritoneal tumor sections from *Amhr2* (CON) and KO (*Amhr2*-KO) mice 10 days after implantation with KPCA cancer cells. Tumor sections were stained by RNAish for *Amhr2*, *Lrrn4*, and *Upk3b* expression. Scale bars, 100 μm.

(E) Cytokine levels in the serum of tumor-bearing mice (N = 5) 10 days after KPCA cells were implanted into *Amhr2*-KO or *Amhr2*^{+/+} (CON) hosts, as measured by the mouse cytokine ELISA array.

(F) IF of PD1 and CTLA4 of KPCA tumor in *Amhr2*-KO mice compared to CON.

(G) Quantification of IF measuring the intensity of signal from PD1 or CTLA4 (green) and normalized by intensity of DAPI (blue), and expression of PD1 and CTLA4 normalized to CD4 expression by qPCR. Data are presented as mean ± SEM; *p < 0.05, **p < 0.01, ***p < 0.001 by t test. n = 3 or more per group. Scale bars, 100 μm.

therefore propose that the AMH/AMHR2 paracrine signaling axis between cancer cells and CAMCs is essential for their pro-tumoral function.

DISCUSSION

In this study we demonstrated that, in ovarian tumors, AMHR2 is primarily expressed by CAMCs of the tumor stroma rather than

by cancer cells, contrary to the long-standing assumptions in the field.^{3,5,9,64} This finding is consistent with the observation that AMHR2 expression is invariably greater in tumors than in ovarian cancer cell lines and explains why AMHR2 expression in ovarian tumors varies by site of metastasis, with greater expression in omental metastases compared to primary tumors.⁶⁵ Furthermore, we showed that cancer cells paradoxically produced AMH,^{12,13} which was otherwise considered to be

anti-tumorigenic.⁹ We therefore speculate that AMH/AMHR2 forms a paracrine axis between cancer cells and CAMCs, whose signaling is important to fine-tune the pro-tumoral functions of CAMCs. This hypothesis could explain the paradoxical findings that both treatments with supraphysiological levels of AMH⁹ or inhibition of AMH signalling with AMH-neutralizing antibodies^{11,12} can inhibit ovarian cancer growth, suggesting both lack of AMH and over-stimulation of this pathway in CAMCs may be detrimental to the growth of the tumor. Moreover, we posit that expression of AMHR2 in CAMCs could explain why it is detected in many other tumor types of non-Müllerian origins with presumably similar mesothelial cell involvement, such as lung, colorectal, and pancreatic cancers.¹⁴ Thus, therapies aimed at this target, such as AMH-neutralizing antibodies, may have applications beyond ovarian cancer in other solid tumor types.

During their frequent dissemination in the peritoneal cavity, ovarian cancer cells are thought to attach to the mesothelium that covers visceral organs, such as the ovary or omentum, and subsequently invade these organs to form a metastasis. During this process, cancer cells presumably reprogram mesothelial cells into CAMCs that envelop the tumor surface and integrate into the tumor stroma, where they are thought to promote cancer growth.^{18,23,29,66,67} To understand the mechanism by which cancer cells reprogram normal mesothelial cells into CAMCs, we performed *in vitro* culture experiments, which revealed that both co-culture with cancer cells and cancer-cell-conditioned medium can induce expression of AMHR2 in primary mesothelial cells isolated from mouse and patient omentum. This expression does not merely represent a marker of CAMC differentiation but plays an important role in the subsequent pro-tumoral function. This was made evident by the fact that experimentally induced overexpression of AMHR2 in Met5a, a normal mesothelial cell line, was sufficient to activate AMH signaling and produce a transcriptional signature consistent with CAMC reprogramming. However, the precise factors secreted by cancer cells that reprogram normal mesothelial cells into CAMCs and induce AMHR2 expression remain unknown but appear herein to be distinct from AMH itself or TGF- β 1, the latter likely regulating other aspects of mesothelial cell function such as EMT.^{57,68} Furthermore, lineage tracing experiments, using a newly developed inducible *Amhr2*-Cre-ERT2 transgenic mouse, revealed important contributions of AMHR2+ cells to the composition of the tumor stroma, suggesting AMHR2+ CAMCs may constitute a stromal progenitor. Thus, the identification of the factors responsible for reprogramming mesothelial cells into CAMCs and the subsequent putative progenitor function of these cells in the tumor stroma should be the subject of future investigations.

An important proposed function of CAMCs is to secrete factors that promote cancer-cell growth.²⁹ Indeed, in our experiments, CAMC-conditioned medium increased proliferation of KPCA cancer cells, and experimental overexpression of AMHR2 in a mesothelial cell line could stimulate both AMHR2+ and AMHR2- cancer-cell lines, suggesting AMHR2 regulates the expression of pro-tumoral growth factors. For example, in Met5a cells, AMHR2 overexpression induced the secretion of growth factors involved in proliferation, migration, and differenti-

ation, such as SPP1, TGF- β superfamily ligands and binding proteins (BMP7, INHBB, INHBA, FSTL3), and ligands of the insulinlike growth factor (IGF) family (IGF1, IGF1, IGL2). Importantly, while the addition of low amounts (1–10 μ g/mL) of exogenous recombinant AMH to CAMC cultures could enhance the mitogenic properties of their secretions on cancer cells, supraphysiological levels (100 μ g/mL) resulted in inhibition of KPCA cancer cells, recapitulating previously reported paradoxical dose-dependent effects,¹² potentially due to the KPCA's baseline expression of low levels of *Amhr2*.

Another proposed function of CAMCs is to promote an immunosuppressive tumor microenvironment to avert tumor immunity.²⁹ The monolayer of mesothelial cells lining the peritoneal cavity forms the first barrier that protects viscera against microorganisms that may invade this space or, in the context of ovarian cancer, cancer cells metastasizing onto peritoneal organs. Peritoneal mesothelium, and particularly that of the omentum, is known to play a role in immunosurveillance; it is capable of displaying antigens on major histocompatibility complex (MHC) class II molecules and secretes cytokines important for the regulation of the innate and adaptive immune systems.^{17,20,28,36} Indeed, mesothelial cells secrete a wide range of cytokines, growth factors, and extracellular matrix (ECM) molecules that directly regulate the recruitment, proliferation, and differentiation of immune cells during inflammation.^{21,26,28} We speculate that cancer cells may use the AMH/AMHR2 signaling axis to modulate existing mesothelial immunomodulatory programs to promote an immunosuppressive tumor microenvironment. In support of this notion, experimental overexpression of AMHR2 in a normal mesothelial cell line was sufficient to reduce the expression of IL1A and IL1B, which promote the migration of inflammatory leukocytes⁶⁹ (Figure 4C). We also observed an increase in the expression of immunosuppressive cytokines IL6, IL20, and IL24, which are frequently overexpressed during ovarian cancer development and mediate a crucial anti-inflammatory role in both local and systemic acute inflammatory responses.^{52–54,70} Furthermore, when mesothelial cells were prompted to differentiate into CAMCs by exposure to cancer-cell-conditioned medium, induction of AMHR2 expression was observed, and modulation of its activity by exogenous AMH could further dynamically regulate the expression of chemoattractant cytokines CCL2, CXCL2, and CXCL3, which control monocyte, neutrophil, macrophage, and dendritic cell infiltration.^{28,46} For example, we observed a significant induction of CCL2 by treating mesothelial cells with cancer-cell-conditioned medium; this cytokine was previously reported to be produced by CAMCs, found to be stimulating the invasion of cancer cells through the MAPK pathway,⁷¹ and could be negatively modulated by high levels of exogenous recombinant AMH, suggesting AMH could serve as a mediator of negative feedback to adjust cytokine secretions. Conversely, AMHR2 overexpression also induced IL6, which is thought to be pro-tumorigenic and immunosuppressive in HGSOV,^{54,72} and this effect was further amplified by addition of exogenous AMH, suggesting positive paracrine feedback. Thus, we hypothesize the AMH-AMHR2 axis may play an important role in fine-tuning cytokine secretions,

which in turn influence immunocyte recruitment and activity within the tumor microenvironment. In this model, AMH secreted by cancer cells in the local tumor microenvironment would dose-dependently modulate the cytokine secretions of CAMCs uniquely expressing its receptor AMHR2. Intriguingly, the presence of AMHR2⁺ mesothelial cells in the ascites of mice and humans with ovarian cancer (Figure 3) suggests CAMCs could also regulate immunocytes in these fluids.

The most striking observation regarding the biological significance of *Amhr2* expression in the tumor stroma was the reduced tumor burden observed when implanting the KPCA cancer cell line into *Amhr2*-KO syngeneic mouse hosts. Indeed, lack of AMHR2 expression in the stroma led to a significantly reduced overall tumor burden and a reduction in metastatic nodule weight, further suggesting that, despite their relatively low abundance, CAMCs may play an important role in tumor growth and dissemination and that AMHR2 expression in CAMCs may be vital to these processes. Moreover, lack of expression of *Amhr2* in mesothelial cells of tumors implanted in KO hosts was sufficient to produce an altered cytokine profile (IL2, IFN γ , IL12p70, CCL3, IL16) in the serum of these mice, despite the relatively low abundance of CAMCs in the tumor microenvironment, presumably by altering the local microenvironment. Many of these cytokines are involved in the Th1 pro-inflammatory pathway important for activating helper CD4⁺ T cells, which could in turn limit tumor development.^{73–76} Moreover, the inhibition of the AMH-AMHR2 axis and altered cytokine secretome was accompanied by a profound and significant reduction of expression of the immune checkpoint proteins PD1 and CTLA4, suggesting a less suppressive immune microenvironment in the absence of AMHR2. These data further support an immunosuppressive function of the AMH-AMHR2 paracrine axis between cancer cells and CAMCs, which may help the tumor evade the host immune system. These results also suggest CAMCs may modulate the infiltration and exhaustion of immune cells in the tumor, particularly at the serosal surface, where they may provide a barrier to peritoneal immunocytes.

Taken together, our study supports the relevance of considering CAMCs as a therapeutic target within the tumor microenvironment. Given the highly restricted somatic expression of AMHR2 to the ovary,⁷⁷ and the mostly post-menopausal HGSOC population, the *de novo* acquisition of expression of AMHR2 in CAMCs may provide a novel therapeutic opportunity to target CAMCs without harming normal peritoneal mesothelium or ovarian function. We speculate that therapeutics targeting AMH/AMHR2, such as with an AMH-neutralizing antibody, or indeed of other pathways critical to CAMC function, may be harnessed to indirectly inhibit cancer-cell growth and metastasis and modulate the tumor immune microenvironment to ameliorate responses to immunotherapies.

Limitation of the study

The study uses a single syngeneic ovarian cancer mouse model (the KPCA model) based on transformed fallopian tube epithelial cell lines in which *Kras*, *P53*, *Ccne1*, and *Akt2* were genetically altered. The findings may not be broadly generalizable to other

cell lines or models carrying different genetic profiles or to cancer cells implanted into hosts from different mouse strains.

The Met5a mesothelial cell line originally derived from the lung may not accurately represent the characteristics of mesothelial cells of omental tissue.

Both the normal human omental tissue and the omental metastases samples used in the study may include patients with differing treatment histories, genetic backgrounds, and histopathologies. These factors could potentially limit the generalizability of the findings.

There may be inherent variability between each sample batch of MPMCs and HPMCs, which could affect the reproducibility of the experimental methods.

The use of a plasmid vector encoding dual expression of *Amhr2v1* and *Acvr1* may introduce artifacts based on ACVR1 overexpression or ignore AMH targets that are dependent on other type I receptor signalling such as BMPR1A or BMPR1B.

STAR★METHODS

Detailed methods are provided in the online version of this paper and include the following:

- KEY RESOURCES TABLE
- RESOURCE AVAILABILITY
 - Lead contact
 - Materials availability
 - Data and code availability
- EXPERIMENTAL MODEL AND SUBJECT DETAILS
 - Human fixed tissue
 - Cell models
 - Mouse models
 - *Amhr2*^{-/-} mice
 - *Amhr2*-Cre-ERT2 x mTmG mice
- METHOD DETAILS
 - Co-culture and conditioned media assay
 - Cancer cell graft
 - Single-cell-RNA-sequencing
 - Bulk-RNaseq
 - *In situ* hybridization
 - Immunofluorescence
 - qPCR
 - Cell viability assay
 - Cytokine array
- QUANTIFICATION AND STATISTICAL ANALYSIS

SUPPLEMENTAL INFORMATION

Supplemental information can be found online at <https://doi.org/10.1016/j.celrep.2023.112730>.

ACKNOWLEDGMENTS

We would like to thank Robert Weinberg for essential comments and suggestions and F. Reinhardt for his help with animal husbandry and treatments. This work was supported by the Assistant Secretary of Defense for Health Affairs through the Ovarian Cancer Research Program under award no. W81XWH-171-0212. The US Army Medical Research Acquisition Activity, 820 Chandler Street, Fort Detrick, MD 21702-5014 is the awarding and administering acquisition office. This work was supported by the central

focus of the Dana-Farber/Harvard Cancer Center (DF/HCC) SPORE in Ovarian Cancer. This work was also supported by the Massachusetts General Hospital Department of Surgery Patricia K. Donahoe, MD, Surgeon-Scientist Research Program: Mid-Career Catalyst Award. The illustrations were created with BioRender.com.

AUTHOR CONTRIBUTIONS

Conceptualization, D.P. and M.C.; methodology, M.C., M.-C.M., S.I., and S.D.; investigation, M.C., D.P., M.-C.M., S.I., R. Mishra, N.M.P.N., P.M., Z.L., N.N., A.K., and S.D.; writing—original draft, D.P. and M.C.; writing—review & editing, D.P., M.C., P.K.D., and D.P.; funding acquisition, D.P.; resources, E.O., C.J.B., R. Maser, J.W., and A.K.M.; supervision, D.P., P.K.D., A.K.M., and C.J.B.

DECLARATION OF INTERESTS

The authors declare no competing interests.

Received: November 23, 2022

Revised: April 27, 2023

Accepted: June 16, 2023

Published: July 14, 2023

REFERENCES

- Moses, M.M., and Behringer, R.R. (2019). A gene regulatory network for Müllerian duct regression. *Environ. Epigenet.* 5, dvz017. <https://doi.org/10.1093/eep/dvz017>.
- Mullen, R.D., and Behringer, R.R. (2014). Molecular genetics of Müllerian duct formation, regression and differentiation. *Sex. Dev.* 8, 281–296. <https://doi.org/10.1159/000364935>.
- Kersual, N., Garambois, V., Chardès, T., Pouget, J.-P., Salhi, I., Bascoul-Mollevis, C., Bibeau, F., Busson, M., Vié, H., Clémenceau, B., et al. (2014). The human Müllerian inhibiting substance type II receptor as immunotherapy target for ovarian cancer. *mAbs* 6, 1314–1326. <https://doi.org/10.4161/mabs.29316>.
- Basal, E., Ayeni, T., Zhang, Q., Langstraat, C., Donahoe, P.K., Pepin, D., Yin, X., Leof, E., and Cliby, W. (2016). Patterns of Müllerian Inhibiting Substance Type II and Candidate Type I Receptors in Epithelial Ovarian Cancer. *Curr. Mol. Med.* 16, 222–231.
- Anttonen, M., Färkkilä, A., Tauriala, H., Kauppinen, M., Maclaughlin, D.T., Unkila-Kallio, L., Bützow, R., and Heikinheimo, M. (2011). Anti-Müllerian hormone inhibits growth of AMH type II receptor-positive human ovarian granulosa cell tumor cells by activating apoptosis. *Lab. Invest.* 91, 1605–1614. <https://doi.org/10.1038/labinvest.2011.116>.
- Gowkielewicz, M., Lipka, A., Majewska, M., Piotrowska, A., Szadurska-Noga, M., Nowakowski, J.J., Wiszpolska, M., Dziegiel, P., Wasniewski, T., Majewski, M.K., and Jozwik, M. (2020). Anti-Müllerian Hormone Type II Receptor Expression in Endometrial Cancer Tissue. *Cells* 9, 2312. <https://doi.org/10.3390/cells9102312>.
- Donahoe, P.K., Swann, D.A., Hayashi, A., and Sullivan, M.D. (1979). Müllerian duct regression in the embryo correlated with cytotoxic activity against human ovarian cancer. *Science* 205, 913–915. <https://doi.org/10.1126/science.472712>.
- Pépin, D., Hoang, M., Nicolaou, F., Hendren, K., Benedict, L.A., Al-Moujahed, A., Sosulski, A., Marmalidou, A., Vavvas, D., and Donahoe, P.K. (2013). An albumin leader sequence coupled with a cleavage site modification enhances the yield of recombinant C-terminal Müllerian Inhibiting Substance. *Technology* 1, 63–71. <https://doi.org/10.1142/S2339547813500076>.
- Pépin, D., Sosulski, A., Zhang, L., Wang, D., Vathipadiekal, V., Hendren, K., Coletti, C.M., Yu, A., Castro, C.M., Birrer, M.J., et al. (2015). AAV9 delivering a modified human Müllerian inhibiting substance as a gene therapy in patient-derived xenografts of ovarian cancer. *Proc. Natl. Acad. Sci. USA* 112, E4418–E4427. <https://doi.org/10.1073/pnas.1510604112>.
- Bougherara, H., Némati, F., Nicolas, A., Massonnet, G., Pugnère, M., Ngô, C., Le Frère-Belda, M.A., Leary, A., Alexandre, J., Meseure, D., et al. (2017). The humanized anti-human AMHRII mAb 3C23K exerts an anti-tumor activity against human ovarian cancer through tumor-associated macrophages. *Oncotarget* 8, 99950–99965. <https://doi.org/10.18632/oncotarget.21556>.
- Estupina, P., Fontayne, A., Barret, J.-M., Kersual, N., Dubreuil, O., Le Blay, M., Pichard, A., Jarlier, M., Pugnère, M., Chauvin, M., et al. (2017). The anti-tumor efficacy of 3C23K, a glyco-engineered humanized anti-MISRII antibody, in an ovarian cancer model is mainly mediated by engagement of immune effector cells. *Oncotarget* 8, 37061–37079. <https://doi.org/10.18632/oncotarget.15715>.
- Chauvin, M., Garambois, V., Colombo, P.-E., Chentouf, M., Gros, L., Brouillet, J.-P., Robert, B., Jarlier, M., Dumas, K., Martineau, P., et al. (2021). Anti-Müllerian hormone (AMH) autocrine signaling promotes survival and proliferation of ovarian cancer cells. *Sci. Rep.* 11, 2231. <https://doi.org/10.1038/s41598-021-81819-y>.
- Chauvin, M., Garambois, V., Choblet, S., Colombo, P.-E., Chentouf, M., Gros, L., De Brauwere, D.-P., Duonor-Cerutti, M., Dumas, K., Robert, B., et al. (2021). Anti-Müllerian hormone concentration regulates activin receptor-like kinase-2/3 expression levels with opposing effects on ovarian cancer cell survival. *Int. J. Oncol.* 59, 43. <https://doi.org/10.3892/ijo.2021.5223>.
- Beck, T.N., Korobeynikov, V.A., Kudinov, A.E., Georgopoulos, R., Solanki, N.R., Andrews-Hoke, M., Kistner, T.M., Pépin, D., Donahoe, P.K., Nicolas, E., et al. (2016). Anti-Müllerian Hormone Signaling Regulates Epithelial Plasticity and Chemoresistance in Lung Cancer. *Cell Rep.* 16, 657–671. <https://doi.org/10.1016/j.celrep.2016.06.043>.
- Iyer, S., Zhang, S., Yucel, S., Horn, H., Smith, S.G., Reinhardt, F., Hoefmit, E., Assatova, B., Casado, J., Meinsohn, M.-C., et al. (2021). Genetically defined syngeneic mouse models of ovarian cancer as tools for the discovery of combination immunotherapy. *Cancer Discov.* 11, 384–407. <https://doi.org/10.1158/2159-8290.CD-20-0818>.
- Shaw, T.J., Zhang, X.Y., Huo, Z., Robertson, D., Lovell, P.A., Dalgleish, A.G., and Barton, D.P.J. (2016). Human Peritoneal Mesothelial Cells Display Phagocytic and Antigen-Presenting Functions to Contribute to Intraperitoneal Immunity. *Int. J. Gynecol. Cancer* 26, 833–838. <https://doi.org/10.1097/IGC.0000000000000697>.
- Ivanov, S., Gallerand, A., Gros, M., Stunault, M.I., Merlin, J., Vaillant, N., Yvan-Charvet, L., and Guinamard, R.R. (2019). Mesothelial cell CSF1 sustains peritoneal macrophage proliferation. *Eur. J. Immunol.* 49, 2012–2018. <https://doi.org/10.1002/eji.201948164>.
- Rynne-Vidal, A., Jiménez-Heffernan, J.A., Fernández-Chacón, C., López-Cabrera, M., and Sandoval, P. (2015). The Mesothelial Origin of Carcinoma Associated-Fibroblasts in Peritoneal Metastasis. *Cancers* 7, 1994–2011. <https://doi.org/10.3390/cancers7040872>.
- Xiang, R., Li, J., Wang, L., and Shi, Y. (2020). Metastatic ovarian cancer shapes the abdominal immune microenvironment by manipulating IL20-IL20RA signaling pathway. *J. Immunol.* 204, 90.6.
- Huang, H., Wang, Z., Zhang, Y., Pradhan, R.N., Ganguly, D., Chandra, R., Murimwa, G., Wright, S., Gu, X., Maddipati, R., et al. (2022). Mesothelial cell-derived antigen-presenting cancer-associated fibroblasts induce expansion of regulatory T cells in pancreatic cancer. *Cancer Cell* 40, 656–673.e7. <https://doi.org/10.1016/j.ccell.2022.04.011>.
- Mutsaers, S.E., Prèle, C.M.A., Pengelly, S., and Herrick, S.E. (2016). Mesothelial cells and peritoneal homeostasis. *Fertil. Steril.* 106, 1018–1024. <https://doi.org/10.1016/j.fertnstert.2016.09.005>.
- López-Cabrera, M. (2014). Mesenchymal Conversion of Mesothelial Cells Is a Key Event in the Pathophysiology of the Peritoneum during Peritoneal Dialysis. *Adv. Met. Med.* 2014, 473134. <https://doi.org/10.1155/2014/473134>.
- Matte, I., Lane, D., Bachvarov, D., Rancourt, C., and Piché, A. (2014). Role of malignant ascites on human mesothelial cells and their gene expression

- profiles. *BMC Cancer* 14, 288. <https://doi.org/10.1186/1471-2407-14-288>.
24. Bilandzic, M., and Stenvers, K.L. (2014). Assessment of Ovarian Cancer Spheroid Attachment and Invasion of Mesothelial Cells in Real Time. *J. Vis. Exp.*, 51655. <https://doi.org/10.3791/51655>.
 25. Mutsaers, S.E. (2002). Mesothelial cells: Their structure, function and role in serosal repair. *Respirology* 7, 171–191. <https://doi.org/10.1046/j.1440-1843.2002.00404.x>.
 26. Mutsaers, S.E., Birnie, K., Lansley, S., Herrick, S.E., Lim, C.-B., and Prèle, C.M. (2015). Mesothelial cells in tissue repair and fibrosis. *Front. Pharmacol.* 6, 113. <https://doi.org/10.3389/fphar.2015.00113>.
 27. Shishido, A., Mori, S., Yokoyama, Y., Hamada, Y., Minami, K., Qian, Y., Wang, J., Hirose, H., Wu, X., Kawaguchi, N., et al. (2018). Mesothelial cells facilitate cancer stem-like properties in spheroids of ovarian cancer cells. *Oncol. Rep.* 40, 2105–2114. <https://doi.org/10.3892/or.2018.6605>.
 28. Mutsaers, S.E., Pixley, F.J., Prèle, C.M., and Hoyne, G.F. (2020). Mesothelial cells regulate immune responses in health and disease: role for immunotherapy in malignant mesothelioma. *Curr. Opin. Immunol.* 64, 88–109. <https://doi.org/10.1016/j.coi.2020.04.005>.
 29. Qian, J., LeSavage, B.L., Hubka, K.M., Ma, C., Natarajan, S., Eggold, J.T., Xiao, Y., Fuh, K.C., Krishnan, V., Enejder, A., et al. (2021). Cancer-associated mesothelial cells promote ovarian cancer chemoresistance through paracrine osteopontin signaling. *J. Clin. Invest.* 131, 146186. <https://doi.org/10.1172/JCI146186>.
 30. Porter, R.L., Sun, S., Flores, M.N., Berzolla, E., You, E., Phillips, I.E., Kc, N., Desai, N., Tai, E.C., Szabolcs, A., et al. (2022). Satellite repeat RNA expression in epithelial ovarian cancer associates with a tumor-immunosuppressive phenotype. *J. Clin. Invest.* 132, e155931. <https://doi.org/10.1172/JCI155931>.
 31. Sosulski, A., Horn, H., Zhang, L., Coletti, C., Vathipadikeal, V., Castro, C.M., Birrer, M.J., Nagano, O., Saya, H., Lage, K., et al. (2016). CD44 Splice Variant v8-10 as a Marker of Serous Ovarian Cancer Prognosis. *PLoS One* 11, e0156595. <https://doi.org/10.1371/journal.pone.0156595>.
 32. DepMap. The Cancer Dependency Map Project at Broad Institute. <https://depmap.org/portal/>.
 33. Kanamori-Katayama, M., Kaiho, A., Ishizu, Y., Okamura-Oho, Y., Hino, O., Abe, M., Kishimoto, T., Sekihara, H., Nakamura, Y., Suzuki, H., et al. (2011). LRRN4 and UPK3B Are Markers of Primary Mesothelial Cells. *PLoS One* 6, e25391. <https://doi.org/10.1371/journal.pone.0025391>.
 34. Chen, Y.-T., Chang, Y.-T., Pan, S.-Y., Chou, Y.-H., Chang, F.-C., Yeh, P.-Y., Liu, Y.-H., Chiang, W.-C., Chen, Y.-M., Wu, K.-D., et al. (2014). Lineage tracing reveals distinctive fates for mesothelial cells and submesothelial fibroblasts during peritoneal injury. *J. Am. Soc. Nephrol.* 25, 2847–2858. <https://doi.org/10.1681/ASN.2013101079>.
 35. Rudat, C., Grieskamp, T., Röhr, C., Airik, R., Wrede, C., Hegermann, J., Herrmann, B.G., Schuster-Gossler, K., and Kispert, A. (2014). Upk3b is dispensable for development and integrity of urothelium and mesothelium. *PLoS One* 9, e112112. <https://doi.org/10.1371/journal.pone.0112112>.
 36. Helmke, A., Nordlohne, J., Balzer, M.S., Dong, L., Rong, S., Hiss, M., Shushakova, N., Haller, H., and von Vietinghoff, S. (2019). CX3CL1-CX3CR1 interaction mediates macrophage-mesothelial cross talk and promotes peritoneal fibrosis. *Kidney Int.* 95, 1405–1417. <https://doi.org/10.1016/j.kint.2018.12.030>.
 37. Zeilemaker, A.M., Mul, F.P., Hoyneck van Papendrecht, A.A., Leguit, P., Verbrugh, H.A., and Roos, D. (1996). Neutrophil adherence to and migration across monolayers of human peritoneal mesothelial cells. The role of mesothelium in the influx of neutrophils during peritonitis. *J. Lab. Clin. Med.* 127, 279–286. [https://doi.org/10.1016/s0022-2143\(96\)90096-7](https://doi.org/10.1016/s0022-2143(96)90096-7).
 38. Han, X., Zhou, Z., Fei, L., Sun, H., Wang, R., Chen, Y., Chen, H., Wang, J., Tang, H., Ge, W., et al. (2020). Construction of a human cell landscape at single-cell level. *Nature* 581, 303–309. <https://doi.org/10.1038/s41586-020-2157-4>.
 39. Izar, B., Tirosh, I., Stover, E.H., Wakiro, I., Cuoco, M.S., Alter, I., Rodman, C., Leeson, R., Su, M.-J., Shah, P., et al. (2020). A single-cell landscape of high-grade serous ovarian cancer. *Nat. Med.* 26, 1271–1279. <https://doi.org/10.1038/s41591-020-0926-0>.
 40. Dasari, S., Pandhiri, T., Grassi, T., Visscher, D.W., Multinu, F., Agarwal, K., Mariani, A., Shridhar, V., and Mitra, A.K. (2020). Signals from the Metastatic Niche Regulate Early and Advanced Ovarian Cancer Metastasis through miR-4454 Downregulation. *Mol. Cancer Res.* 18, 1202–1217. <https://doi.org/10.1158/1541-7786.MCR-19-1162>.
 41. Ray, U., Jung, D.-B., Jin, L., Xiao, Y., Dasari, S., Sarkar Bhattacharya, S., Thirusangu, P., Staub, J.K., Roy, D., Roy, B., et al. (2022). Targeting LRR15 Inhibits Metastatic Dissemination of Ovarian Cancer. *Cancer Res.* 82, 1038–1054. <https://doi.org/10.1158/0008-5472.CAN-21-0622>.
 42. Jullien, N., Goddard, I., Selmi-Ruby, S., Fina, J.-L., Cremer, H., and Herman, J.-P. (2008). Use of ERT2-iCre-ERT2 for conditional transgenesis. *Genesis* 46, 193–199. <https://doi.org/10.1002/dvg.20383>.
 43. Kristianto, J., Johnson, M.G., Zastrow, R.K., Radcliff, A.B., and Blank, R.D. (2017). Spontaneous recombinase activity of Cre-ERT2 in vivo. *Transgenic Res.* 26, 411–417. <https://doi.org/10.1007/s11248-017-0018-1>.
 44. Lechner, J.F., Tokiwa, T., LaVeck, M., Benedict, W.F., Banks-Schlegel, S., Yeager, H., Banerjee, A., and Harris, C.C. (1985). Asbestos-associated chromosomal changes in human mesothelial cells. *Proc. Natl. Acad. Sci. USA* 82, 3884–3888. <https://doi.org/10.1073/pnas.82.11.3884>.
 45. Imhoff, F.M., Yang, D., Mathew, S.F., Clarkson, A.N., Kawagishi, Y., Tate, W.P., Koishi, K., and McLennan, I.S. (2013). The type 2 anti-Müllerian hormone receptor has splice variants that are dominant-negative inhibitors. *FEBS Lett.* 587, 1749–1753. <https://doi.org/10.1016/j.febslet.2013.04.014>.
 46. Kadomoto, S., Izumi, K., and Mizokami, A. (2021). Roles of CCL2-CCR2 Axis in the Tumor Microenvironment. *Int. J. Mol. Sci.* 22, 8530. <https://doi.org/10.3390/ijms22168530>.
 47. De Filippo, K., Dudeck, A., Hasenberg, M., Nye, E., van Rooijen, N., Hartmann, K., Gunzer, M., Roers, A., and Hogg, N. (2013). Mast cell and macrophage chemokines CXCL1/CXCL2 control the early stage of neutrophil recruitment during tissue inflammation. *Blood* 121, 4930–4937. <https://doi.org/10.1182/blood-2013-02-486217>.
 48. Reyes, N., Figueroa, S., Tiwari, R., and Geliebter, J. (2021). CXCL3 Signaling in the Tumor Microenvironment. In *Tumor Microenvironment: The Role of Chemokines – Part B Advances in Experimental Medicine and Biology*, A. Birbrair, ed. (Springer International Publishing), pp. 15–24. https://doi.org/10.1007/978-3-030-62658-7_2.
 49. Van Den Eeckhout, B., Tavernier, J., and Gerlo, S. (2020). Interleukin-1 as Innate Mediator of T Cell Immunity. *Front. Immunol.* 11, 621931. <https://doi.org/10.3389/fimmu.2020.621931>.
 50. Dinarello, C.A. (2018). Overview of the IL-1 family in innate inflammation and acquired immunity. *Immunol. Rev.* 281, 8–27. <https://doi.org/10.1111/imr.12621>.
 51. Yazdi, A.S., and Ghoreschi, K. (2016). The Interleukin-1 Family. *Adv. Exp. Med. Biol.* 941, 21–29. https://doi.org/10.1007/978-94-024-0921-5_2.
 52. Xing, Z., Gaudie, J., Cox, G., Baumann, H., Jordana, M., Lei, X.F., and Achong, M.K. (1998). IL-6 is an antiinflammatory cytokine required for controlling local or systemic acute inflammatory responses. *J. Clin. Invest.* 101, 311–320. <https://doi.org/10.1172/JCI1368>.
 53. Fujino, S., Yokoyama, A., Kohno, N., and Hiwada, K. (1996). Interleukin 6 is an autocrine growth factor for normal human pleural mesothelial cells. *Am. J. Respir. Cell Mol. Biol.* 14, 508–515. <https://doi.org/10.1165/ajrcmb.14.6.8652179>.
 54. Offner, F.A., Obrist, P., Stadlmann, S., Feichtinger, H., Klingler, P., Herold, M., Zwierzina, H., Hittmair, A., Mikuz, G., and Abendstein, B. (1995). IL-6 secretion by human peritoneal mesothelial and ovarian cancer cells. *Cytokine* 7, 542–547. <https://doi.org/10.1006/cyto.1995.0073>.

55. Kumari, N., Dwarakanath, B.S., Das, A., and Bhatt, A.N. (2016). Role of interleukin-6 in cancer progression and therapeutic resistance. *Tumour Biol.* 37, 11553–11572. <https://doi.org/10.1007/s13277-016-5098-7>.
56. Wei, H., Li, B., Sun, A., and Guo, F. (2019). Interleukin-10 Family Cytokines Immunobiology and Structure. In *Structural Immunology Advances in Experimental Medicine and Biology*, T. Jin and Q. Yin, eds. (Springer), pp. 79–96. https://doi.org/10.1007/978-981-13-9367-9_4.
57. Kenny, H.A., Chiang, C.-Y., White, E.A., Schryver, E.M., Habis, M., Romero, I.L., Ladanyi, A., Penicka, C.V., George, J., Matlin, K., et al. (2014). Mesothelial cells promote early ovarian cancer metastasis through fibronectin secretion. *J. Clin. Invest.* 124, 4614–4628. <https://doi.org/10.1172/JCI74778>.
58. Jamin, S.P., Arango, N.A., Mishina, Y., Hanks, M.C., and Behringer, R.R. (2002). Requirement of Bmpr1a for Müllerian duct regression during male sexual development. *Nat. Genet.* 32, 408–410. <https://doi.org/10.1038/ng1003>.
59. Rosenberg, S.A. (2014). IL-2: the first effective immunotherapy for human cancer. *J. Immunol.* 192, 5451–5458. <https://doi.org/10.4049/jimmunol.1490019>.
60. Mirlekar, B., and Pylayeva-Gupta, Y. (2021). IL-12 Family Cytokines in Cancer and Immunotherapy. *Cancers* 13, 167. <https://doi.org/10.3390/cancers13020167>.
61. Alspach, E., Lussier, D.M., and Schreiber, R.D. (2019). Interferon γ and Its Important Roles in Promoting and Inhibiting Spontaneous and Therapeutic Cancer Immunity. *Cold Spring Harbor Perspect. Biol.* 11, a028480. <https://doi.org/10.1101/cshperspect.a028480>.
62. Ntanasis-Stathopoulos, I., Fotiou, D., and Terpos, E. (2020). CCL3 Signaling in the Tumor Microenvironment. *Adv. Exp. Med. Biol.* 1231, 13–21. https://doi.org/10.1007/978-3-030-36667-4_2.
63. McFadden, C., Morgan, R., Rahangdale, S., Green, D., Yamasaki, H., Center, D., and Cruikshank, W. (2007). Preferential migration of T regulatory cells induced by IL-16. *J. Immunol.* 179, 6439–6445. <https://doi.org/10.4049/jimmunol.179.10.6439>.
64. Segev, D.L., Hoshiya, Y., Hoshiya, M., Tran, T.T., Carey, J.L., Stephen, A.E., MacLaughlin, D.T., Donahoe, P.K., and Maheswaran, S. (2002). Mullerian-inhibiting substance regulates NF- κ B signaling in the prostate in vitro and in vivo. *Proc. Natl. Acad. Sci. USA* 99, 239–244. <https://doi.org/10.1073/pnas.221599298>.
65. Sallinen, H., Janhonen, S., Pölonen, P., Niskanen, H., Liu, O.H., Kivelä, A., Hartikainen, J.M., Anttila, M., Heinäniemi, M., Ylä-Herttuala, S., and Kaikkonen, M.U. (2019). Comparative transcriptome analysis of matched primary and distant metastatic ovarian carcinoma. *BMC Cancer* 19, 1121. <https://doi.org/10.1186/s12885-019-6339-0>.
66. Abe, T., Ohuchida, K., Koikawa, K., Endo, S., Okumura, T., Sada, M., Horioka, K., Zheng, B., Moriyama, T., Nakata, K., et al. (2017). Cancer-associated peritoneal mesothelial cells lead the formation of pancreatic cancer peritoneal dissemination. *Int. J. Oncol.* 50, 457–467. <https://doi.org/10.3892/ijo.2016.3829>.
67. Mogi, K., Yoshihara, M., Iyoshi, S., Kitami, K., Uno, K., Tano, S., Koya, Y., Sugiyama, M., Yamakita, Y., Nawa, A., et al. (2021). Ovarian Cancer-Associated Mesothelial Cells: Transdifferentiation to Minions of Cancer and Orchestrate Developing Peritoneal Dissemination. *Cancers* 13, 1352. <https://doi.org/10.3390/cancers13061352>.
68. Yoshihara, M., Kajiyama, H., Yokoi, A., Sugiyama, M., Koya, Y., Yamakita, Y., Liu, W., Nakamura, K., Moriyama, Y., Yasui, H., et al. (2020). Ovarian cancer-associated mesothelial cells induce acquired platinum-resistance in peritoneal metastasis via the FN1/Akt signaling pathway. *Int. J. Cancer* 146, 2268–2280. <https://doi.org/10.1002/ijc.32854>.
69. Schunk, S.J., Triem, S., Schmit, D., Zewinger, S., Sarakpi, T., Becker, E., Hütter, G., Wrublewsky, S., Küting, F., Hohl, M., et al. (2021). Interleukin-1 α Is a Central Regulator of Leukocyte-Endothelial Adhesion in Myocardial Infarction and in Chronic Kidney Disease. *Circulation* 144, 893–908. <https://doi.org/10.1161/CIRCULATIONAHA.121.053547>.
70. Topley, N., Jörres, A., Luttmann, W., Petersen, M.M., Lang, M.J., Thierach, K.H., Müller, C., Coles, G.A., Davies, M., and Williams, J.D. (1993). Human peritoneal mesothelial cells synthesize interleukin-6: induction by IL-1 beta and TNF alpha. *Kidney Int.* 43, 226–233. <https://doi.org/10.1038/ki.1993.36>.
71. Yasui, H., Kajiyama, H., Tamauchi, S., Suzuki, S., Peng, Y., Yoshikawa, N., Sugiyama, M., Nakamura, K., and Kikkawa, F. (2020). CCL2 secreted from cancer-associated mesothelial cells promotes peritoneal metastasis of ovarian cancer cells through the P38-MAPK pathway. *Clin. Exp. Metastasis* 37, 145–158. <https://doi.org/10.1007/s10585-019-09993-y>.
72. Kampan, N.C., Madondo, M.T., Reynolds, J., Hallo, J., McNally, O.M., Jobling, T.W., Stephens, A.N., Quinn, M.A., and Plebanski, M. (2020). Pre-operative sera interleukin-6 in the diagnosis of high-grade serous ovarian cancer. *Sci. Rep.* 10, 2213. <https://doi.org/10.1038/s41598-020-59009-z>.
73. Chen, Q., Ghilardi, N., Wang, H., Baker, T., Xie, M.-H., Gurney, A., Grewal, I.S., and de Sauvage, F.J. (2000). Development of Th1-type immune responses requires the type I cytokine receptor TCCR. *Nature* 407, 916–920. <https://doi.org/10.1038/35038103>.
74. Zhang, Y., Zhang, Y., Gu, W., He, L., and Sun, B. (2014). Th1/Th2 cell's function in immune system. *Adv. Exp. Med. Biol.* 841, 45–65. https://doi.org/10.1007/978-94-017-9487-9_3.
75. Xu, H.-M. (2014). Th1 cytokine-based immunotherapy for cancer. *Hepatobiliary Pancreat. Dis. Int.* 13, 482–494. [https://doi.org/10.1016/s1499-3872\(14\)60305-2](https://doi.org/10.1016/s1499-3872(14)60305-2).
76. Szabo, S.J., Sullivan, B.M., Peng, S.L., and Glimcher, L.H. (2003). Molecular mechanisms regulating Th1 immune responses. *Annu. Rev. Immunol.* 21, 713–758. <https://doi.org/10.1146/annurev.immunol.21.120601.140942>.
77. Meinsohn, M.-C., Saatcioglu, H.D., Wei, L., Li, Y., Horn, H., Chauvin, M., Kano, M., Nguyen, N.M.P., Nagyker, N., Kashiwagi, A., et al. (2021). Single-cell sequencing reveals suppressive transcriptional programs regulated by MIS/AMH in neonatal ovaries. *Proc. Natl. Acad. Sci. USA* 118, e2100920118. <https://doi.org/10.1073/pnas.2100920118>.
78. Macosko, E.Z., Basu, A., Satija, R., Nemesh, J., Shekhar, K., Goldman, M., Tirosh, I., Bialas, A.R., Kamitaki, N., Martersteck, E.M., et al. (2015). Highly Parallel Genome-wide Expression Profiling of Individual Cells Using Nanoliter Droplets. *Cell* 161, 1202–1214. <https://doi.org/10.1016/j.cell.2015.05.002>.

STAR★METHODS

KEY RESOURCES TABLE

REAGENT or RESOURCE	SOURCE	IDENTIFIER
Antibodies		
P-SMAD1/5 (Ser463/465) (41D10) rabbit MAb antibody	Cell Signaling Technology	Cat# 9516; RRID:AB_491015
UPK3B Polyclonal antibody	ProteinTech	Cat# 15709-1-AP; RRID:AB_2878170
LRRN4 Polyclonal Antibody	ThermoFisher	Cat# PA5-33910; RRID:AB_2551278
MISR II Antibody (D-9)	Santa Cruz	Cat#sc-377413
MIS-R2 Antibody #4518	Cell Signaling Technology	Cat# 4518; RRID:AB_2258236
β-Actin (13E5) Rabbit mAb	Cell Signaling Technology	Cat# 4970; RRID:AB_2223172
InVivoPlus anti-mouse PD-1	BioXcell	Cat# BE0273; RRID:AB_2687796
CTLA-4 Antibody (F-8)	Santa Cruz Biotechnology	Cat# sc-376016; RRID:AB_10988256
Alpha-Smooth Muscle Actin Monoclonal Antibody (1A4)	ThermoFisher	Cat# MA1-06110; RRID:AB_557419
Vimentin (D21H3) XP® Rabbit mAb	Cell Signaling Technology	Cat# 5741; RRID:AB_10695459
Biological samples		
Mouse KPCA Tumors	S. Iyer et al. ¹⁵	N/A
Chemicals, peptides, and recombinant proteins		
LR-AMH	D. Pepin et al. ⁸	N/A
Recombinant mouse TGFβ1	R&D system	#7754-BH
Recombinant human TGFβ1	R&D system	#7666-MB
Collagenase	Milipore-Sigma	# 10103578001
Hyaluronidase	Milipore-Sigma	#H3506
DNAse	Milipore-Sigma	# 11284932001
Zeocin	InVivoGen	#ant-zn-05
Fugene6	Promega	#E2692
Tamoxifen vivo	Milipore-Sigma	# 5648-1G
Tamoxifen vitro (4-OHT)	Milipore-Sigma	#H6278
Critical commercial assays		
CellTiter-Glo® Luminescent Cell Viability Assay	Promega	#G7570
Deposited data		
Western blot	This paper	https://doi.org/10.17632/6xwgzcbd28.1
Origine code	This paper	https://doi.org/10.5281/zenodo.7967478
KPCA tumor and ascite raw and analyzed data	This paper	GEO: GSE233423
Bulk RNA seq	This paper	GEO: GSE236657
Mouse omentum raw data and analyzed	Han X et al. ³⁸	GEO: GSE134355
Human ascites raw data and analyzed	Izar B et al. ³⁹	GEO: GSE146026
Experimental models: Cell lines		
KPCA	MIT Whitehead Institute	Sonia Iyer - Robert Weinberg laboratory
OV90	ATCC	CRL-11732
MET5A	ATCC	RRID:CVCL_3749
KURAMOCHI	Japanese Collection of Research Bioresources	RRID:CVCL_1345

(Continued on next page)

Continued		
REAGENT or RESOURCE	SOURCE	IDENTIFIER
HPMC	Female human donors Indiana University School of Medicine	N/A
MPMC	Mice omentum In this paper	N/A
AM	Isolated from patients' ascites Massachusetts General Hospital	N/A
AY	Isolated from patients' ascites Massachusetts General Hospital	N/A
BI	Isolated from patients' ascites Massachusetts General Hospital	N/A
Experimental models: Organisms/strains		
WT mice	Jackson Laboratory	RRID:IMSR_JAX:000664
AMHR2KO mice	Mutant Mouse Regional Resource Centers (MMRRC)	B6; 129S7-Amhr2tm3(cre)Bhr/Mmnc, backcrossed with C57BL/6J
Amhr2-CRE-ERT2	Jackson Laboratory	N/A
Rosa26 CRE-inducible mTmG reporter	Jackson Laboratory	N/A
Oligonucleotides		
AMHR2 Forward (Genotyping – AMHR2KO mice)	Invitrogen	N/A
AMHR2 Reverse (Genotyping – AMHR2KO mice)	Invitrogen	N/A
AMHR2 Forward (Genotyping - Amhr2-CRE-ERT2 mice)	Invitrogen	N/A
AMHR2 Reverse (Genotyping - Amhr2-CRE-ERT2 mice)	Invitrogen	N/A
Mouse & Human IL1B, CCL2, CXCL2, CXCL3, IL6, CD44, SPP1, AMHR2, AMH, LRNN4, UPK3B	IDT design	N/A
RNAscope 2.5 HD Detection Kit	Advanced Cell Diagnostics, ACD	Cat No. 322350
RNAscope™ 2.5 HD Duplex Assay	Advanced Cell Diagnostics, ACD	Cat No. 322430
Probe mAmhr2	Advanced Cell Diagnostics, ACD	Cat No. 489821
Probe mLrrm4	Advanced Cell Diagnostics, ACD	Cat No. 443951
Probe mUpk3b	Advanced Cell Diagnostics, ACD	Cat No. 568561
Probe mMsln	Advanced Cell Diagnostics, ACD	Cat No. 443241
Probe mWt1	Advanced Cell Diagnostics, ACD	Cat No. 432711
Probe hAMHR2	Advanced Cell Diagnostics, ACD	Cat No. 490241
Probe hLRRN4	Advanced Cell Diagnostics, ACD	Cat Ni. 1030591
Probe hUPK3B	Advanced Cell Diagnostics, ACD	Cat No. 581091
Recombinant DNA		
pCDNA 3.1-AMHR2v1	Genscript	N/A
pCDNA 3.1-AMHR2v3	Genscript	N/A
Software and algorithms		
CellProfiler Image Analysis Software	SciCrunch Registry	RRID:SCR_007358)
GraphPad – Prism	SciCrunch Registry	RRID:SCR_002798
Rstudio	SciCrunch Registry	RRID:SCR_000432

RESOURCE AVAILABILITY

Lead contact

Further information and requests should be directed to the lead contact, David Pépin (Dpepin@mgh.harvard.edu).

Materials availability

Requests for resources and reagents should be directed to, and will be fulfilled, by the [lead contact](#).

Data and code availability

- Single-cell RNA-seq data generated in this study have been deposited at Gene Expression Omnibus with the accession number GEO: GSE233423. Accession numbers are listed in the [key resources table](#). Original western blot images have been deposited at Mendeley with the accession number Mendeley Data: <https://data.mendeley.com/datasets/6xwzgcbdd28/1>. The DOI is listed in the [key resources table](#). Microscopy data reported in this paper will be shared by the [lead contact](#) upon request.
- All original code has been deposited at Zenodo and is publicly available as of the date of publication. DOIs are listed in the [key resources table](#).
- Any additional information required to reanalyze the data reported in this paper is available from the [lead contact](#) upon request.

EXPERIMENTAL MODEL AND SUBJECT DETAILS

Human fixed tissue

Human sections of high-grade serous ovarian cancer (HGSO) tumors and normal omental tissue from female donors were generously donated by the Massachusetts General Hospital, the Gynecological Pathology Department. These donations were made in accordance with an IRB-approved protocol (2007P001918).

Cell models

The KPCA cell lines were developed and described in Iyer et al.¹⁵ and the OV90 cells lines of malignant papillary serous adenocarcinoma from ATCC. These cells were cultured in DMEM medium supplemented with 1% of FBS and 1% penicillin and streptomycin and incubated at 37°C.

The Met5a cell line was purchased from ATCC and cultured in DMEM medium supplemented with 10% FBS. Met5a were stably transfected with plasmids encoding the active (pCDNA 3.1-AMHR2v1-T2A-ACVR1) or inactive (pCDNA 3.1-AMHR2v3-T2A-ACVR1) splice variants of AMHR2.⁴⁵ Transfections were performed using Fugene6 reagents according to the manufacturer (Promega) instructions, and 3 validated stably expressing clones were used in subsequent experiments. These clones were selected and cultured in presence of 100µg/ml of zeocin to maintain selection.

Kuramochi cell were obtained from the Japanese Collection of Research Bioresources.

HPMC were isolated from omentum from female human donors as described previously⁴⁰ and cultured in DMEM with 10% FBS, 1% MEM non-essential amino acids, 1% MEM vitamins, and 1% penicillin and streptomycin.

MPMC were obtained from the omentum of female mice by mechanically disrupting small pieces and performing enzymatic digestion using collagenase, hyaluronidase, and DNase at 37°C for 45 min. The pieces of tissue were placed in a collector tube in a gentlemacs dissociator (Miltenyi). The resulting cell suspension was filtered through a 70 µm filter and washed 3 times with PBS (Phosphate Buffer Saline). Pellet was resuspended with ACK (Ammonium Chloride Potassium) lysis buffer to lyse red blood cells at room temperature for 10 min and washed with PBS. The adherent cells were cultivated in DMEM:F12 medium, supplemented with 10% of FBS (Fetal Bovine Serum) and 1% of penicillin/streptomycin.

The primary human ovarian cancer cells (BI, AY, AM), were collected from ascites of deidentified patient after informed consent under Institutional Review Board-approved protocols (2007P001918/Massachusetts General Hospital) as part of a previous study.⁹ The adherent cells were cultivated in DMEM:F12, supplemented with 10% of FBS and 1% of penicillin/streptomycin.

Mouse models

This study was performed according to experimental protocols 2009N000033, approved by the Massachusetts General Hospital Institutional Animal Care and Use Committee with C57BL/6J mice purchased from the Jackson Laboratory.

Amhr2^{-/-} mice

Amhr2-Cre knock-in mice were purchased from the Mutant Mouse Regional Resource Centers (MMRRC) (strain B6; 129S7-Amhr2tm3(cre)Bhr/Mmnc, backcrossed with C57BL/6J).⁵⁸ Ear genotyping of the Amhr2-Cre knock-in and WT mice were done with REExtract-N-Amp Tissue PCR Kit (Sigma) with a previously described sets of primers.⁵⁸ Only female mice carrying the Amhr2-Cre knock-in allele were used in this study.

Amhr2-Cre-ERT2 x mTmG mice

Amhr2-Cre-ERT2 were developed in collaboration with the Jackson Laboratory. Briefly, they are the result of a knock-in of a CRE-ER fusion transgene in frame with the Amhr2 gene using a T2 exon skipping mechanism to ensure Amhr2 expression is maintained. These mice were then crossed with the Rosa26 CRE-inducible mTmG reporter as previously described.^{42,43} Ear genotyping of Amhr2-Cre-ERT2 and mTmG reporter mice were done using the REExtract-N-Amp tissue PCR kit (Sigma, #SLBT8193) with sets of primers design by IDT and Invitrogen ([key resources table](#)). Tamoxifen (4-OHT, Sigma-Aldrich) treatment was used to induce

Cre-ER nuclear translocation, at a final concentration of 2 μ M *in vitro* in female mesothelial cells isolated from omenta as described above. Only female mice carrying the *Amhr2-Cre-ERT2* x mTmG were used in this study.

METHOD DETAILS

Co-culture and conditioned media assay

Mouse Primary Mesothelial cells (MPMC) and the murine ovarian cancer cells KPCA were co-cultured for 48h in a 6-well plate at ratio of 1:1 (3.10⁵ cells each) in DMEM supplemented with 1% of FBS. *Amhr2* expression was analyzed by qPCR on the pool of cells (MPMC+KPCA) and the fold change was normalized to each cell type non-mixed assuming 1:1 composition and thus a geometric average of their expression when combined.

Likewise, the human Primary Mesothelial cell (HPMC) were cultivated with the human ovarian cancer cell line Kuramochi for 48h in a 6 well plate at ratio of 1:1 (3.10⁵ cells each) in DMEM supplemented with 1% of FBS. The Kuramochi and HPMC cells in co-culture were separated by flow cytometry based on GFP expression in the Kuramochi as previously described by Dasari et al.⁴⁰ RNA was isolated using miRNeasy kit (Qiagen) and gene expression was measured independently in each cell type by qPCR.

For the cancer-cell conditioned medium, the cancer cell lines using in this study was (OV90, BI, KPCA) were grown in DMEM supplemented with 1% FBS, for 48h. The conditioned media was centrifuged to ensure removal of cells and the cell-free supernatant was added to the mesothelial cells (MPMC or HPMC) for 48h or unconditioned media as a control.

Cancer cell graft

Female mice were injected with 5.10⁶ cells of KPCA intraperitoneally and sacrificed after 14 days to evaluate tumor burden. Tumors were visualized by UV illumination and fluorescence, based on GFP expression in KPCA cells, at the time of dissection.

Single-cell-RNA-sequencing

Single cell RNA sequencing was performed with 10x Genomics kit following manufacturer instructions, on tumors from different clones of KPCA cancer cells including KPCA.A, KPCA.B, and KPCA.C¹⁵ (N = 4 pooled tumors per genotype) and cells from peritoneal fluid. We isolated 5000 cells per sample and loaded them for single cell analysis. The data analysis was performed using Cell Ranger (version 3.1.0) with standard parameters. Samples were aligned against the refdata-gex-mm10-2020-A reference sequences and were analyzed using Seurat⁷⁸ (R version 4.1.2 - Seurat version 4.1.1) as previously described by Iyer et al.¹⁵ Standard pre-processing workflow was applied independently to each sample. Samples were filtered for mitochondrial percentage <20% and unique feature counts over 200 and less than 8000. Samples were normalized then merged using “merge” function in Seurat. Standard parameters for visualization and clustering were performed throughout the analysis. Markers for each level of cluster were identified using FindAllMarkers in Seurat. The 10X scRNAseq dataset of KPCA.A, KPCA.B, and KPCA.C tumors and KPCA.C ascites is available on Gene Expression Omnibus (GEO) platform under accession number GEO: GSE233423.

Bulk-RNAseq

RNA was extracted from cell lines using the Qiagen RNA extraction kit according to the manufacturer's instructions. Library construction, sequencing, and analysis was performed by Novogene Corporation Inc. In brief, alignments were performed using HISAT2 to the human reference Homo Sapiens (GRCh38/hg38). Genes with adjusted p value <0.05 and |log₂(FoldChange)| > 1 were considered as differentially expressed. Genes listed in [Table S1](#): RNA sequencing performed on Met5a cells overexpressing two variants of the *Amhr2* receptor: *Amhr2-v3*, which is an inactive receptor, and *Amhr2-v1*, which is an active receptor. Genes listed in [Table S2](#): RNA sequencing of KPCA tumors derived from wild-type mice *Amhr2+/(CON)*, *Amhr2+/-* (*Amhr2-HET*) and *Amhr2 -/-* knock-out mice (*Amhr2-KO*). The bulk RNAseq dataset is available on the GEO platform under accession number GEO: GSE236657.

In situ hybridization

Tumors and omenta were fixed in 10% neutral buffered formalin at room temperature and were embedded in paraffin blocks in an automated tissue processor (Leica). Blocks were sectioned at 10 μ m thickness and stained with hematoxylin and the RNA scope (ACD Bio) system. Briefly, we used the RNAscope 2.5 HD Detection Kit (Advanced Cell Diagnostics, ACD) for the in-situ Hybridization of mouse and human *Amhr2*, (ACD, m-489821; h-490241), *Lrrm4* (ACD, m-443951; h-1030591), *Upk3b* (ACD, m-588561; h-581091), *Wt1* (ACD, m-432711), *Msln* (ACD, 443141) according to the manufacturer's instructions for formalin-fixed paraffin-embedded tissue sections.

Immunofluorescence

The immunofluorescence staining was performed fixed cells and permeabilized with Triton X-100 (0.1%). The cells were incubated for 1 h in blocking buffer at room temperature, followed by three washes with PBS. Then, the cells were incubated with the primary antibody for 2 h or overnight at 4°C, with the antibody concentration as recommended by the manufacturer. The cells were washed and incubated for 1 h with the specific secondary antibody. To visualize the stained proteins, the cells were counterstained with the Dapi nuclear stain 5 min and a final wash step with PBS. The coverslips were mounted onto glass slides using Vectashield mounting medium to preserve the fluorescence signal.

qPCR

Total RNA was extracted from cancer or mesothelial cells using the Qiagen RNA extraction kit, and cDNA was synthesized from total RNA using SuperScript III First-Strand Synthesis System for RT-PCR (Invitrogen). Expression levels relative to the geometric mean housekeeping genes were calculated by using cycle threshold (Ct) values logarithmically transformed using the $2^{-\Delta Ct}$ function.

Cell viability assay

For cell viability/proliferation assays, we used the CellTiter-Glo Luminescent Cell Viability Assay system (Promega) according to the manufacturer's instructions. Briefly, 1.10^4 cells were plated in each well of a 96-well plate and cultured in 100 μ L DMEM/F-12/1% FBS medium overnight. Cells were then incubated with media conditioned (48h) by Met5a clones stably expressing *AMHR2v1* or *AMHR2v3*, or MPMC, or CAMC cells (MPMC previously treated for 72h with KPCA media). Cells were grown for 72h, then 20 μ L of CellTiter-Glo Luminescent solution reagent was added per well, and plates were incubated in a humidified incubator until the positive control wells became brown (from 1 to 2 h, depending on the cell line). Then, absorbance was measured at 490 nm using a spectrophotometer microplate reader. Three replicate wells were used for each condition.

Cytokine array

Cytokines levels were measured in the serum of tumor-bearing mice (N = 5) 10 days after KPCA cells were implanted into *Amhr2^{-/-}* or *Amhr2^{+/+}* wild-type hosts. Serum was run in duplicate in the mouse cytokine 44-plex panel from Eve Technology[®]. Values out of range of the standard curve were not included.

QUANTIFICATION AND STATISTICAL ANALYSIS

Statistical analysis was performed using GraphPad Prism 9.5.1 software (GraphPad Software, Inc. RRID:SCR_002798), using an independent sample t test unless otherwise indicated or ANOVA test. $p \leq 0.05$ was considered as significant. Data are represented as mean \pm standard error of the mean (SEM).

CellProfiler version 4.2.5 Software (available at www.cellprofiler.org), was used to quantify signal intensity by using the following pipeline: the merged color pictures with DAPI in blue and CTLA4 or PD1 in green were split between these two channels and each one was converted to gray. Based on DAPI images the tissue was manually delimited and the intensity of each staining was quantified. The ratio between CTLA4 or PD1 and DAPI signals was calculated, and the average value of the controls was normalized to 1 while the *Amhr2^{-/-}* sample intensities were calculated relative to control values.